Check for updates

Received: 24 February 2025 | Accepted: 16 July 2025

DOI: 10.1111/1365-2745.70147

BRITISH ECOLOGICAL SOCIETY Journal of Ecology

RESEARCH ARTICLE

Biomass production of tropical trees across space and time: The shifting roles of diameter growth and wood density

Bruna Hornink[1,2] | Pieter A. Zuidema[3] | Peter van der Sleen[3] | Amy E. Zanne[4] | Gabriel Assis-Pereira[2,5] | Daigard Ricardo Ortega Rodriguez[2] | Claudia Fontana[2,6] | Leif Armando Portal-Cahuana[7] | Edilson Jimmy Requena-Rojas[8,9] | Ana Carolina Maioli Campos Barbosa[10] | Daniela Granato-Souza[11] | Lucas Guimarães Pereira[10] | Claudio Sergio Lisi[12] | Itallo Romany Nunes Menezes[12] | Alejandro Venegas-Gonzalez[13] | Nelson Jaén-Barrios[1,14] | Fidel A. Roig[15,16] | Mario Tomazello-Filho[2] | Peter Groenendijk[1]

Correspondence
Bruna Hornink
Email: bhornink@gmail.com

Funding information
Fundação de Amparo à Pesquisa do Estado de São Paulo, Grant/Award Number: 2009/53951-7, 2017/50085-3, 2018/01847-0, 2018/22914-8, 2019/22516-5, 2019/26350-4, 2023/07753-6 and 2023/14668-5; Coordenação de Aperfeiçoamento de Pessoal de Nível Superior, Grant/Award Number: 88887.975357/2024-00; Fundação de Amparo à Pesquisa do Estado de Minas Gerais, Grant/Award Number: APQ-01544-22; ITTO, Grant/Award Number: 046/12S; Conselho Nacional de Desenvolvimento Científico e Tecnológico, Grant/Award Number: 160852/2022-6, 2024/14406-3 and 403596/2023-8

Handling Editor: Toby Jackson

Abstract

1. Woody biomass in tropical trees contributes significantly to global carbon stocks; however, these stocks are increasingly affected by climate and land-use changes. Understanding the growth mechanisms driving woody biomass production is essential for assessing the short- and long-term contributions to carbon stocks and dynamics in tropical forests.
2. Trees accumulate biomass by increasing their size (wood volume) and/or tissue density (wood density). However, estimates of tree biomass production are often based solely on size increment through measurements of stem diameter growth, overlooking the potential spatial and temporal variation in wood density within trees. Tree-ring analysis can be applied to reconstruct past tree volume-growth and wood-density variations, allowing the quantification of their relative contributions when reconstructing past woody biomass production.
3. Here, we studied trees of the widespread Neotropical genus *Cedrela* along an environmental (climate and soil) gradient to address two key questions: (1) How does temporal variation in tree diameter growth and wood density affect biomass production? (2) To what extent do these relationships vary along the environmental gradient? We examined both long-term (ontogenetic) and short-term (annual) variations in diameter growth and wood density, covering eighteen sites in the Amazon rainforest, Atlantic Forest, Cerrado savanna and Caatinga dry forest.
4. We found that diameter growth and wood density drive short- and long-term biomass production dynamics. Interestingly, diameter growth patterns predominantly explained short-term variability in biomass production at all sites,

For affiliations refer to page 13.

This is an open access article under the terms of the Creative Commons Attribution License, which permits use, distribution and reproduction in any medium, provided the original work is properly cited.
© 2025 The Author(s). *Journal of Ecology* published by John Wiley & Sons Ltd on behalf of British Ecological Society.

whereas wood density explained ontogenetic biomass patterns mainly at humid sites. These results highlight the importance of accounting for both short- and long-term variation, including climatic and ontogenetic drivers, to increase the accuracy of biomass estimations in tropical trees, particularly in humid forest ecosystems such as the Amazon.

5. *Synthesis*. Diameter growth is an important and good indicator of forest carbon production. However, size-related changes in wood density, which are usually neglected, are critical for accurate short- and long-term carbon assessments, especially in tropical humid sites.

KEYWORDS
Cedrela, dendrochronology, environmental gradient, interannual variation, ontogeny, plant–climate interactions, tree-ring

1 | INTRODUCTION

Tropical forests are essential to the global carbon cycle, accounting for two-thirds of the terrestrial woody biomass (Pan et al., 2013) and more than half of the world's aboveground forest carbon (Pan et al., 2024). Trees store ~40%–50% of carbon in their dry biomass across their lifespan (Martin & Thomas, 2011), serving as long-term carbon reservoirs (Köhl et al., 2017). However, climate change and land-use intensification threaten tropical tree biomass dynamics in the short- and long-term (Bauman et al., 2022; Locosselli et al., 2020; Mitchard, 2018). Predicting future carbon budgets in these forests requires a mechanistic understanding of the factors driving biomass production and carbon stocks in trees, which remain understudied at temporal and spatial scales (Zuidema et al., 2013).

Tree biomass production is a complex process shaped by the morphology and functioning of xylem cells responsible for wood formation (Lachenbruch & McCulloh, 2014), reflecting resource allocation, mechanical and hydraulic architecture, defence mechanisms (Philipson et al., 2014) and respiratory and maintenance costs (Anten & Schieving, 2010). However, studies assessing biomass production often use the relatively easy-to-measure tree's diameter growth from permanent sample plots to reconstruct tree volumetric growth (Banin et al., 2014; Chave et al., 2003). While this metric provides valuable insights, it fails to capture total biomass gain, as it overlooks the role of species-specific variations in the density of woody tissue within the tree size-related progress across space and time (Mo et al., 2024).

In recent years, wood density has been recognised as a critical aspect of tree biomass production (Baker et al., 2004; Chave et al., 2014; Phillips et al., 2019). Wood density reflects species-specific acquisitive (low density, fast growth) to conservative (high density, slow growth) growth strategies (Chave et al., 2009; Reich, 2014) and is modulated by local environmental conditions such as precipitation, temperature, soil fertility and soil water content (Muller-Landau, 2004; Poorter et al., 2017). Critically, wood density also varies within individuals over time, responding to both long-term ontogenetic trends (e.g. increasing density with tree size; Bastin et al., 2015; González-Melo, 2021) and short-term annual climatic fluctuations (e.g. annual precipitation and temperature; Ortega Rodriguez, Sánchez-Salguero, Hevia, Granato-Souza, Assis-Pereira, et al., 2023; Pompa-García et al., 2024).

Short- and long-term variations in wood density across temporal and spatial scales add complexity to the reconstruction and evaluation of tree biomass production. Given that trees accumulate growth over time in their cross-sections, it is possible to reconstruct the ontogenetic and annual variation in tree diameter growth (Groenendijk et al., 2017; López & Fontana, 2024) and wood density (Gonçalves et al., 2021; Köhl et al., 2017; Ortega Rodriguez, Sánchez-Salguero, Hevia, Granato-Souza, Assis-Pereira, et al., 2023) using dendrochronological techniques (Babst et al., 2014; Fritts, 1976; Groenendijk et al., 2025).

Here, we applied dendrochronology and X-ray densitometry techniques to study the roles of short- and long-term variation in diameter growth and wood density in driving biomass production shifts for a widespread tropical genus: *Cedrela* spp. (Meliaceae). This genus was selected due to its extensive distribution across various forest types and its responsiveness to local climatic conditions (Fontana et al., 2024; Granato-Souza et al., 2019; Menezes et al., 2022; Venegas-González et al., 2018) that allow us to assess tree growth in diverse forest ecosystems. We addressed two key questions: (1) How does temporal variation (ontogenetic and annual) in tree diameter growth and wood density affect biomass production? and (2) To what extent do these responses vary along an environmental gradient (climate and soil)? We expect that temporal variations in diameter growth and wood density, driven by size-related factors (long-term) and interannual conditions (short-term), significantly contribute to biomass production along the climate gradient, with stronger effects observed in resource-rich environments.

2 | MATERIALS AND METHODS

2.1 | Sample collection

Samples were collected from eighteen forest sites across Brazil and Peru, covering a range of forest types and environmental characteristics (Figure 1, Table 1, Tables S1 and S2). The study sites included national, state and municipal parks and private forests located in

13652745, 0, Downloaded from https://besjournals.onlinelibrary.wiley.com/doi/10.1111/1365-2745.70147 by Cochrane Peru, Wiley Online Library on [01/09/2025]. See the Terms and Conditions (https://onlinelibrary.wiley.com/terms-and-conditions) on Wiley Online Library for rules of use; OA articles are governed by the applicable Creative Commons License

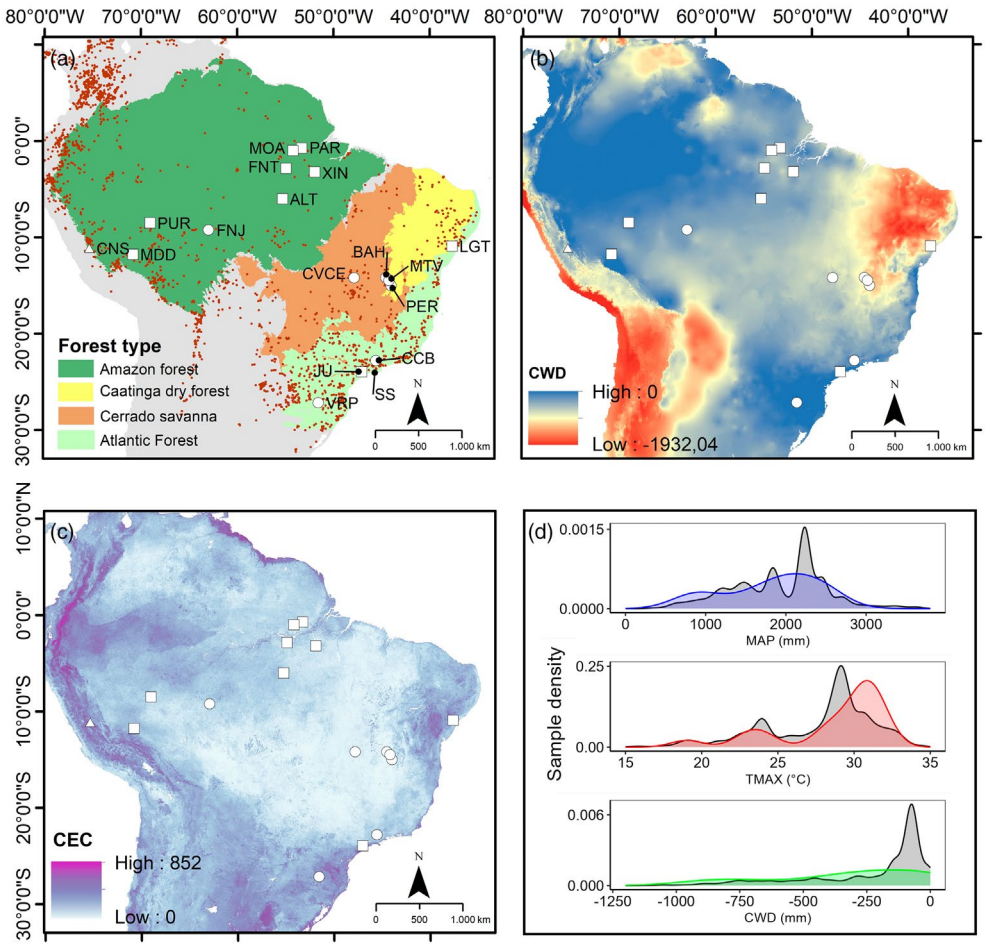

FIGURE 1 (a) Location of the study sites (shapes) and the neotropical geographical distribution of the genus *Cedrela* (small brown dots; based on the GBIF database: GBIF.org, 2024). (b) Distribution of study sites under the annual water stress gradient, expressed in Climatic Water Deficit gradient (CWD is the difference between monthly rainfall and monthly evapotranspiration, from Chave et al., 2014). It is a measure of water stress, where more negative values indicate greater soil water deficit and higher stress for plants). (c) Distribution of study sites under the soil fertility gradient: Expressed in terms of Cation Exchange Capacity (CEC; SoilGrids 2.0; from ISRIC—World Soil Information—soilgrids.org; Poggio et al., 2021): Represents the amount of positive charge that can be exchanged per mass of soil. (d) Kernel density estimates of climate data for the entire neotropical distribution of the genus *Cedrela* P. Browne (black line; extracted from GBIF 2024, 17,898 records with valid coordinates) and the distribution of our 18 sampling sites (coloured line), for Mean Annual Precipitation (MAP) and Mean Maximum Temperature (Tmax), both from TerraClimate, from 1991 to 2020 (Abatzoglou et al., 2018) and Climatic Water Deficit (CWD), from Chave et al. (2014). Species: *Cedrela fissilis* Vell. (circles), *Cedrela odorata* L. (squares) and *Cedrela montana* Moritz ex Turcz. (triangles).

tropical and subtropical regions (Table S1). These sites represent ecosystems from the Amazon Rainforest, Atlantic Forest, Brazilian Cerrado savanna and Caatinga dry forest (Table 1 and Figure 1a). Samples from sites in the Amazon were collected in sustainable-use conservation units (National and State Forests), where legal forest management operations are conducted. In these areas, samples were obtained by collecting cross-sectional wedges from felled trees as part of authorised logging activities. It is important to note that harvesting operations occur in native forests without prior management. In the remaining areas, samples were collected from state, municipal and private forests where forest management is not legally authorised. In these cases, non-destructive coring methods were used to extract wood samples. Fieldwork permits were obtained from environmental authorities where required (e.g. SISBIO in Brazil; see authorisation numbers in Table S1). In forest concession areas, authorisation was previously granted to the forest management company responsible for the concession. On privately owned land, sampling was conducted with prior authorisation from the landowner.

Each population was sampled in different years for various dendrochronological applications (dendroecology, dendroclimatology and forest management, Table 1). Additional details about each site can be found in published studies and unpublished theses (Table S1—Reference). To maintain consistency in our sampling methodology, we included only samples that spanned from the pith to the bark, contained the pith or were close enough to estimate the distance to the pith. At each location, the number of trees we used ranged from eight to eighteen, due to the availability of samples with complete pith and sufficient material for wood density analysis.

13652745, 0, Downloaded from https://besjournals.onlinelibrary.wiley.com/doi/10.1111/1365-2745.70147 by Cochrane Peru, Wiley Online Library on [01/09/2025]. See the Terms and Conditions (https://onlinelibrary.wiley.com/terms-and-conditions) on Wiley Online Library for rules of use; OA articles are governed by the applicable Creative Commons License

TABLE 1 *Cedrela* spp. population features and local characteristics.

Site	Vegetation	Climate	Species	Chron	*N*	Year of collection	Mean TRW	Mean WD	Mean ABP	Mean age
ALT	Ombrophilous Dense Forest	Am	CO	n	10	2017	4.72 ± 2.49	0.39 ± 0.08	36.4 ± 39.1	54.3 ± 17.1
BAH	Dry forest	Aw	CF	n	11	2017	3.67 ± 3.07	0.56 ± 0.09	19.29 ± 18.3	56 ± 13.91
CCB	Ombrophilous Dense Forest	Cf	CO	y	8	2015	2.79 ± 1.96	0.51 ± 0.08	10.62 ± 9.89	49.25 ± 9.5
CNS	Montane forest	Bw	CM	y	10	2009–2010	5.26 ± 3.41	0.45 ± 0.08	109.3 ± 119.6	88.6 ± 43.41
CVCE	Dry forest	Aw	CF	y	10	2023	2.84 ± 2.39	0.55 ± 0.08	16.2 ± 23.1	55.9 ± 23.53
FNJ	Ombrophilous Open Forest	Am	CF	y	10	2019	2.53 ± 1.37	0.42 ± 0.06	24.4 ± 21.8	114.2 ± 32.54
FNT	Ombrophilous Dense Forest	Am	CO	y	15	2013–2015	2.48 ± 1.92	0.4 ± 0.08	20.3 ± 21.7	113.4 ± 25.03
JU	Ombrophilous Dense Forest	Cf	CF	y	10	2016	2.42 ± 2.11	0.52 ± 0.1	9.05 ± 14.09	55.5 ± 14.68
LGT	Dry forest	As	CO	y	18	2022	2.23 ± 1.6	0.51 ± 0.13	6.68 ± 8.17	65.83 ± 28.17
MDD	Ombrophilous Dense Forest	Af	CO	y	9	2018	2.22 ± 1.56	0.4 ± 0.07	22.3 ± 23.3	138.11 ± 28.45
MOA	Ombrophilous Dense Forest	Af	CO	n	8	2017	1.34 ± 1.14	0.41 ± 0.08	10.96 ± 15.5	202.5 ± 90.86
MTV	Dry forest	Aw	CF	y	10	2016	1.6 ± 1.34	0.47 ± 0.1	4.03 ± 6.55	68 ± 30.25
PAR	Ombrophilous Dense Forest	Am	CO	y	9	2017	2.43 ± 1.74	0.44 ± 0.07	25.9 ± 29.3	127.11 ± 76.8
PER	Dry forest	Aw	CF	y	13	2017	1.95 ± 2.02	0.52 ± 0.11	10 ± 14.5	102.77 ± 38.9
PUR	Ombrophilous Dense Forest	Aw	CO	n	10	2021	3.13 ± 2.53	0.45 ± 0.08	38.93 ± 46	102 ± 33.02
SS	Ombrophilous Dense Forest	Cf	CO	y	9	2016	4.08 ± 2.85	0.54 ± 0.07	25.05 ± 31.6	43.33 ± 9.46
VRP	Mixed Ombrophilous Forest	Cf	CF	y	15	2019	2.65 ± 2.03	0.42 ± 0.09	7.4 ± 8.16	60.8 ± 20.66
XIN	Ombrophilous Dense Forest	Am	CO	n	10	2016	2.11 ± 1.95	0.42 ± 0.08	20.1 ± 30.1	125.2 ± 40.09

Note: Site: Population identity. Climate: Aw = equatorial winter dry, Cf = warm temperature fully humid, Am = equatorial monsoonal, As = equatorial steppe, Bw = arid desert. Species: CF = *Cedrela fissilis*, CO = *Cedrela odorata* and CM = *Cedrela montana*. Chron: y = there is a tree-ring width chronology available; n = there is no tree-ring width chronology available. *N* = number of trees at each site. Mean TRW = average tree-ring width, in mm. Mean WD = average tree-ring basic wood density, in g/cm^3. Mean ABP = mean absolute annual biomass production, in kg. Mean age = average maximum age within the population in years. For all variables, we provided the means with standard deviations.

13652745, 0, Downloaded from https://besjournals.onlinelibrary.wiley.com/doi/10.1111/1365-2745.70147 by Cochrane Peru, Wiley Online Library on [01/09/2025]. See the Terms and Conditions (https://onlinelibrary.wiley.com/terms-and-conditions) on Wiley Online Library for rules of use; OA articles are governed by the applicable Creative Commons License

2.2 | Genus *Cedrela*

In this study, we focused on three *Cedrela* species: *Cedrela odorata* L., *Cedrela fissilis* Vell. and *Cedrela montana* Moritz ex Turcz. *Cedrela* is a genus widely distributed throughout the Neotropics (Pennington et al., 2010). Among these species, *C. odorata* and *C. fissilis* are the most common in a variety of forest types ranging from humid to dry forests, typically in areas with well-drained soils (Pennington et al., 2010). In Brazil, these species are found in the Caatinga (sensu stricto), Cerrado (sensu lato), riparian or gallery forest, terra firme forest, floodplain forest, deciduous seasonal forest, evergreen seasonal forest, semi-deciduous seasonal forest and ombrophilous forest (Flores, 2021). *Cedrela* species are typically described as semi-deciduous or deciduous trees, losing their leaves partially or completely during the dry season (Marcati et al., 2006; Mendivelso et al., 2016). Studies have shown a direct relationship between leaf expansion, radial growth and wood density, with cambial dormancy occurring during the dry season (Andreacci et al., 2017; Mendivelso et al., 2016). *C. fissilis* and *C. odorata* are usually described as fast-growing species (Pennington et al., 2010; Tomazello Filho et al., 2000) while *C. montana* is described as slow-growing (Bräuning et al., 2009). *Cedrela* reaches different diameters and heights depending on the environment. For example, *C. odorata* and *C. fissilis* can reach heights of 25–40 m and diameters of 60–150 cm in areas with annual precipitation between 2500 and 4000 mm (Tomazello Filho et al., 2000). In contrast, in drier regions, these species generally have diameters under 60 cm and heights of 10–20 m (Brienen et al., 2010).

In *Cedrela* species, growth rings are reliably annual (Baker et al., 2017), characterised by marginal parenchyma bands associated with semi-porous or porous xylem, and such structures are well defined via X-ray densitometry (Tomazello Filho et al., 2000). The annual nature of ring formation and response to climate in *Cedrela* species has been well demonstrated across a wide range of forests, including the Amazon (Granato-Souza et al., 2019; Ortega Rodriguez, Sánchez-Salguero, Hevia, Granato-Souza, Assis-Pereira, et al., 2023), high mountain (Bräuning et al., 2009), Atlantic (Fontana et al., 2024; Venegas-González et al., 2018) and dry (Menezes et al., 2022; Pagotto et al., 2021) forests. One exception occurs in Suriname, where *C. odorata* forms two rings per year under a bimodal annual rainy season (Baker et al., 2017). The reliability of measurable rings of known frequency makes *Cedrela* an ideal model for studying tree-ring growth across various forest ecosystems, offering insights into the ecological mechanisms that drive short- and long-term biomass production in tropical trees.

2.3 | Sample preparation and wood density analyses

We selected one radius from each tree to perform the analyses (Table 1). All the cores were previously polished and scanned at high resolution (1200–2400 dpi); tree rings were marked following the marginal parenchyma bands associated with semi-porous or porous xylem.

To measure growth rates and wood density, cores were sectioned transversely into radial sections of 0.5–2 cm wide and 1.5 mm thick, while wedges were cut into sections of 2 cm wide and 1.5 mm thick. Wood density was determined following the protocol established by Quintilhan et al. (2021) and Tomazello et al. (2009). Radial sections were conditioned in a climatic chamber at 20°C and 60% relative humidity until they reached a stable moisture content of 12%. All samples were scanned in an X-ray densitometry chamber (Faxitron X-Ray, Illinois, USA) equipped with a measurement unit scale and a cellulose acetate calibration wedge for wood density calibration. Digital X-ray images of the radial section samples (96 dpi, .tiff) were analysed with WinDendro Density 2017a® software (Regent Instruments Inc., Canada) to obtain the tree-ring width (TRW) and tree-ring wood density at 12% moisture content ($WD_{U12\%}$) per year. Sample preparation, X-ray imaging and wood density measurements were performed at the Tree-Ring and Wood Anatomy Laboratory of the University of São Paulo (Piracicaba, São Paulo—Brazil). Data processing and data analysis were conducted at the Dendroecology and Wood Biology Laboratory at the State University of Campinas—UNICAMP (Campinas, São Paulo—Brazil).

2.4 | Diameter reconstruction and biomass estimation

For each tree, the cumulative diameter (*D*) and cumulative basal area (BA) during the year of ring formation were reconstructed by summing the subsequent tree-ring widths from pith to bark, assuming a circular growth pattern. For tree-ring samples without a visible pith, we estimated the missing distance based on the concentric circle method in CDendro and CooRecorder® software.

To calculate the aboveground biomass production per year, we first reconstructed the total historical aboveground biomass per year (B) using the pantropical equation described by Chave et al. (2014) (Equation 1). Not all sites had tree height data available; therefore, we used the pantropical equation that included a diameter–height allometric model. This model has a stress factor (*E*, Table S2) that represents the environmental conditions of the site where the trees grow. Chave et al. (2014) demonstrated that factor *E* is strongly dependent on the diameter–height allometry relationship and is particularly useful for improving model accuracy in the absence of tree height data.

For each tree and year, biomass was estimated based on *D* and a tree-level weighted average wood density (WD_{WA}). The WD_{WA} value was obtained from the weighted average of the $WD_{U12\%}$ values by the basal area increment of each year (Equation 2). This calculation was designed to prevent the influence of the wood proportion near the pith (Williamson & Wiemann, 2010). Before weighing, $WD_{U12\%}$ was transformed into basic wood density (WD) by multiplying $WD_{U12\%}$ by 0.838 (Vieilledent et al., 2018).

13652745, 0, Downloaded from https://besjournals.onlinelibrary.wiley.com/doi/10.1111/1365-2745.70147 by Cochrane Peru, Wiley Online Library on [01/09/2025]. See the Terms and Conditions (https://onlinelibrary.wiley.com/terms-and-conditions) on Wiley Online Library for rules of use; OA articles are governed by the applicable Creative Commons License

The absolute ABP was obtained by subtracting the total biomass from the present year minus the total biomass of the previous year ($ABP = B_t - B_{t-1}$). We also calculated the relative change in biomass per year by dividing the ABP from the present year by the total biomass from the previous year ($ABP_P = ABP_t/B_{t-1}$) to reduce the size-ABP relationship bias.

$$B = \exp\left[-18.03 - 0.976E + 0.976\ \ln(WD_{WA}) + 2.673\ \ln(D) - 0.0299\left[\ln(D)^2\right]\right] \quad (1)$$

where B is the historical aboveground biomass (kg); D is the total diameter of each tree per year reconstructed by the accumulated tree-ring width increment (cm); WD_{WA} is the average basic wood density weighted by basal area increment (g/cm^3); E is the environmental stress factor unitless for each site obtained from the raster file available in Chave et al. (2014).

$$WD_{WA} = \sum_{t=1}^{n} \frac{BAIt * WDt}{BAt} \quad (2)$$

where WD_{WA} is the weighted average wood density (g/cm^3); BAIt is the basal area increment in year t (m^2); WD is the basic wood density (g/cm^3), obtained from $WD_{U12\%}$ * 0.838 in year t; BAt is the total basal area in year t (m^2).

2.5 | Environmental data

Studies have shown that rainfall patterns (Mendivelso et al., 2016), photoperiod and temperature (Andreacci et al., 2017) drive the cambial activity of *Cedrela* species and that precipitation levels during the dry season (Zuidema et al., 2022) mainly contribute to diameter growth of tropical species. Based on these relationships, we tested nine climatic variables: Mean Annual Total Precipitation (MAP, mm), Mean Annual Precipitation of the Wettest Quarter (MAPqmax, mm), Mean Annual Precipitation of the Driest Quarter (MAPqmin, mm), Mean Annual Maximum Temperature (TMAX, °C), Mean Annual Minimum Temperature (TMIN, °C), Mean Annual Vapour Pressure Deficit total (VPD, kPa), Mean Annual Solar Radiation total (SRAD, W/m^2) and Climatic Water Deficit (CWD, mm). Except for CWD, climatic variables were obtained for each *Cedrela* spp. population from TerraClimate, considering the historical temporal extension from 1991 to 2020 (Abatzoglou et al., 2018) (Table S2). CWD was obtained for each site from the raster available by Chave et al. (2014), representing the difference between rainfall and evapotranspiration during dry months in mm/year, when evapotranspiration exceeds rainfall.

Additionally, soil fertility has been reported to influence biomass production (Van Der Sande et al., 2018), leading to variation even between the western and eastern Amazon Basin (Quesada et al., 2012). High soil fertility is linked to a near-neutral pH (5.5–7.5), high soil organic carbon, clay fraction and cation exchange capacity (CEC) (Brady & Weil, 2016). pH tends to optimise nutrient availability and minimises the toxicity of elements such as aluminium and manganese. SOC improves soil structure, moisture retention and the supply of essential nutrients to plants. Clay fraction influences the soil's capacity to retain water and nutrients, whereas CEC reflects the soil's potential to store and provide essential cations such as calcium, magnesium and potassium. Based on this, we tested four soil variables: pH measured in water (pH, H_2O), soil organic carbon (SOC, g/kg), clay content (Clay, %) and cation exchange capacity (CEC, cmolc/kg), extracted from the international soil database—SoilGrids (Poggio et al., 2021), at three depths: 0–5, 5–15 and 15–30 cm. We used a weighted mean to average the values between 0 and 30 cm (e.g. average soil values = pH 0–5 cm × 5/30 + pH 5–15 cm × 10/30 + pH 15–30 cm × 15/30). For two sites (MTV and BAH) that were too close to urban areas and were not available in the SoilGrids database, we used the National Soil Profile Database for Brazil available to international scientists (Cooper et al., 2005; Muniz et al., 2011), also considering 0–30 cm depth (Table S2).

2.6 | Data analysis

Prior to analyses, TRW, WD, ABP, ABP_P and D values were log-transformed to reduce skewness in their distributions. Subsequently, all variables were standardised per site (mean-centred and scaled by their standard deviations) to facilitate the comparison of the effect sizes. We operationally defined ontogeny as long-term changes in TRW, WD, ABP and ABP_P associated with size-dependent developmental stages (Hérault et al., 2011). Thus, we quantified ontogenetic changes using the cumulative diameter (D) per tree to reflect the progression of the developmental stage. This approach is justified because (i) our samples have a strong relationship between age and diameter growth (see Table S3, Figure S11), potentially due to the fast growth and light-demanding behaviour of *Cedrela* (Peters et al., 2015) and (ii) size rather than age is often a better predictor of an individual's ontogenetic stage in tropical forests (Groenendijk et al., 2017; King et al., 2005).

2.6.1 | Diameter growth and wood density effect on biomass production

To answer the first question, we investigated the relationships among TRW, WD, ABP, ABP_P and D over time, conducting a path analysis per site using structural equation modelling (Shipley, 2016; Figure 2 and Figure S12). The path analysis allowed us to partition the total ontogenetic effect on biomass production (ABP and ABP_P) into direct and indirect effects mediated by TRW and WD (Figure 2). The analysis was conducted by employing generalised linear mixed-effects models (GLMMs) (Equation 3, Table S4; Zuur et al., 2009). These models can account for the repeated measurement and the hierarchical structure of the data (trees within sites). Individual tree identity interacting with site (site: tree) was

13652745, 0, Downloaded from https://besjournals.onlinelibrary.wiley.com/doi/10.1111/1365-2745.70147 by Cochrane Peru, Wiley Online Library on [01/09/2025]. See the Terms and Conditions (https://onlinelibrary.wiley.com/terms-and-conditions) on Wiley Online Library for rules of use; OA articles are governed by the applicable Creative Commons License

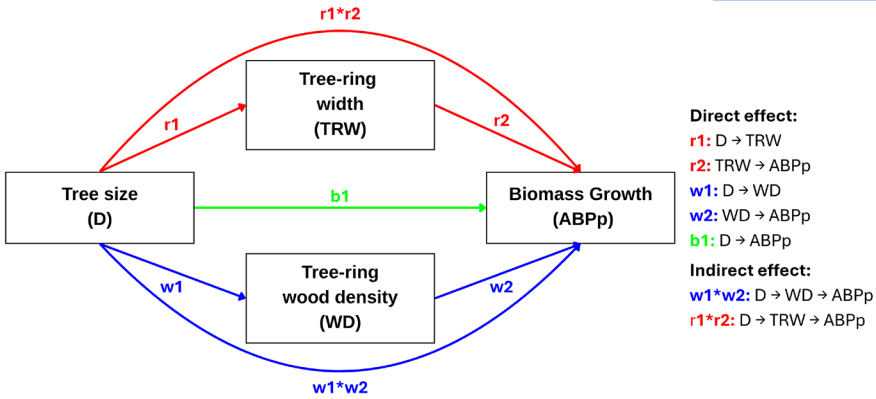

FIGURE 2 Structural diagram of the path analysis model showing the hypothesised relationships between tree size (*D*), tree-ring width (TRW), wood density (WD) and relative biomass production (ABP_P). Arrows indicate direct and indirect pathways with standardised coefficients. The model accounts for long-term ontogenetic effect (tree size) and short-term variation in tree-ring and wood density. Direct effects represent the immediate influence of one variable on another (r1, r2, w1, w2, b1). Indirect effects represent the influence of one variable on another mediated by one or more intermediate variables and are calculated as the product of the path coefficients (r1 × r2, w1 × w2). Direct effect: Tree size effect on ABP_P (b1), TRW (r1) and WD (w1); TRW effect on ABP_P (r2) and WD effect on ABP_P (w2). Indirect effects: Tree size effect via TRW (r1 × r2) and WD (w1 × w2). The total effect is the sum of direct and indirect effects (b1 + r1 × r2 + w1 × w2).

included as a random intercept, allowing us to model the unique growth trajectories of each tree. The predictors *D*, WD and TRW were included as a random slope, allowing their effects on biomass production to vary among individual trees. The models were fitted using restricted maximum likelihood, which optimises the likelihood estimation under fixed effects while considering the variability of random effects. The proportion of variance explained by the fixed effects alone and by the entire model, including random effects, was quantified by the marginal and conditional R^2, respectively (Nakagawa & Schielzeth, 2013).

To derive site-level representations of the direct and indirect effects, we extracted the random slopes (pathway estimates) associated with each tree within each site (Site: Tree) and then computed their mean per site. The direct ontogenetic effect of *D* on TRW, WD and ABP or ABP_P was represented by r1, w1 and b1, respectively. The direct interannual effect of TRW and WD on ABP or ABP_P was quantified by r2 and w2, respectively. We used a complete model to quantify r2, w2 and b1. This approach allowed us to simultaneously control the impact of each variable (Equation 3 iii). By including random effects to capture differences among trees within a site, the model facilitated the explanation of total variability and minimised residual error, resulting in more robust and comprehensive conclusions about the factors influencing ABP or ABP_P. The indirect ontogenetic effect via TRW and WD was calculated as the product of the path coefficients along the mediated pathways, representing the ontogenetic effect via TRW and WD on ABP or ABP_P. The indirect effect of diameter via TRW was computed as r1 × r2, and the indirect effect via WD was w1 × w2. The total ontogenetic effect of *D* was the sum of the direct effect of diameter on ABP and the indirect effects through TRW and WD.

$$\text{(i)}\ TRW_{ijk} = \beta_0 + \beta_1 D_{ijk} + u_{0ij} + u_{1ij} D_{ijk} + \epsilon_{ijk}$$

$$\text{(ii)}\ WD_{ijk} = \beta_0 + \beta_1 D_{ijk} + u_{0ij} + u_{1ij} D_{ijk} + \epsilon_{ijk}$$

$$\text{(iii)}\ ABP_{Pijk} = \beta_0 + \beta_1 TRW_{ijk} + \beta_2 WD_{ijk} + \beta_3 D_{ijk} + u_{0ij} + u_{1ij} TRW_{ijk} + u_{2ij} WD_{ijk} + u_{3ij} D_{ijk} + \epsilon_{ijk} \quad (3)$$

where ABP_P is the proportion of aboveground biomass production; TRW_{ijk} is the tree-ring width; WD_{ijk} is the tree-ring wood density; D_{ijk} is the accumulated diameter, all measured for the *k*-th year of the *j*-th tree in the *i*-th site. β_0 is the fixed intercept. β_1 is the fixed effect coefficient for diameter in model (i) and (ii). β_1, β_2 and β_3 are the fixed effect coefficients for tree-ring width (TRW), wood density (WD) and diameter (*D*) in model (iii), respectively. u_{0ij} is the random intercept for the *j*-th tree within the *i*-th site. u_{1ij}, u_{2ij}, and u_{3ij} are the random slopes for TRW, WD and *D* for the *j*-th tree within the *i*-th site. ϵ_{ijk} is the residual error for the *k*-th year for the *j*-th tree in the *i*-th site. All values were log-transformed to reduce skewness in their distributions and were standardised per site.

All analyses were performed using both ABP and ABP_P. As ABP_P reduces size-related bias, its results are presented in the main text, while ABP results are available in Supporting Information (Figures S12 and S13, Table S5).

2.6.2 | Association with climatic characteristics

Further, to address the second question, we used bootstrap correlation tests to assess the statistical significance and robustness of the relationships between the direct and indirect effects and the climatic and soil conditions at each site. By resampling the data with replacement (1000 bootstrap iterations), we generated empirical distributions of the correlation coefficients. Additionally, we performed linear regression analyses to quantify the strength and direction of

13652745, 0, Downloaded from https://besjournals.onlinelibrary.wiley.com/doi/10.1111/1365-2745.70147 by Cochrane Peru, Wiley Online Library on [01/09/2025]. See the Terms and Conditions (https://onlinelibrary.wiley.com/terms-and-conditions) on Wiley Online Library for rules of use; OA articles are governed by the applicable Creative Commons License

the relationships between the effects derived from the path analysis (direct and indirect effects) and the interaction between climatic variables and soil condition at each site.

All statistical analyses were conducted using R software (version 4.4.1; R Core Team, 2022). The following packages were used: *piecewiseSEM* (Lefcheck, 2016) for running the path analysis; *lme4* (Bates et al., 2015) for fitting linear mixed-effects models; *boot* (Canty & Ripley, 1999) for performing bootstrap resampling and calculating bootstrap statistics; and *ggplot2* (Wickham, 2016) for data visualisation.

3 | RESULTS

3.1 | Tree-ring width, wood density and biomass production

Across sites, we observed variation in the mean WD, TRW and the absolute and relative annual biomass (ABP and ABP_P) (Figure 3 and Figure S1). Mean WD ranged from $0.39 \pm 0.08\,g/cm^3$ (ALT) to $0.56 \pm 0.09\,g/cm^3$ (BAH) with relatively low variability within sites (ranging from FNJ with 2.28 to PER 5.41-fold change, Figures S2 and S3). In contrast, mean TRW ranged from 1.34 ± 1.14 mm (MOA) to 5.26 ± 3.41 mm (CNS), showing substantial variability within sites (ranging from FNJ with 72.13 to CNS with 1196.77-fold change, Figures S4 and S5). Mean ABP ranged from 4.03 ± 6.55 kg/year (MTV) to 109 ± 119 kg/year (CNS), and mean ABP_P ranged from 0.1 ± 0.19 (CNS) to 0.64 ± 5.52 (CVCE). Both presented the highest temporal and spatial variation (>600-fold variation, Figures S6–S9).

Sites in dry forests and transition zones had the highest WD values, ranging from $0.47 \pm 0.1\,g/cm^3$ (MTV) to $0.56 \pm 0.09\,g/cm^3$ (BAH), but the lowest TRW, ranging from 1.60 ± 1.34 mm (MTV) to 3.67 ± 3.07 mm (BAH), and the lowest ABP, ranging from 4.08 ± 6.55 kg (MTV) to 19.29 ± 18.3 kg (BAH) (Figure 3 and Figure S1). In contrast, sites in the western Amazon and Atlantic Forest had the highest TRW, achieving 5.26 ± 3.41 mm with *C. montana* (CNS). Amazonian sites exhibited the highest ABP (over $20\,kg\,year^{-1}$), but also the lowest ABP_P ($<0.10\,year^{-1}$). This suggests that trees produce large amounts of biomass annually but exhibit low relative growth rates when scaled to total biomass. In contrast, both the transition zones (e.g. LGT, CVCE) and the wettest Atlantic Forest (e.g. JU, SS) sites showed lower ABP ($<10\,kg\,year^{-1}$), yet consistently higher ABP_P (from $0.15–0.64\,year^{-1}$). This suggests that although trees in these regions produce less biomass in absolute terms, they grow rapidly when scaled to total biomass. A summary of the statistical differences among sites and species is provided in Supporting Information (II).

3.2 | Effect of tree size, tree-ring width and wood density on biomass production

The path analysis revealed significant relationships between tree size and its direct effect on TRW (r1: r^2 cond. = 0.27, p-value < 0.001) and WD (w1: r^2 cond. = 0.61, p-value < 0.001) (Figure 4, Table S5). The direct path coefficient r1 was, in general, significantly negative (r1 = −0.16), ranging from −0.36 (FNT) to 0.08 (PUR) across sites (Figure 4a). This result suggests that larger trees tend to produce narrower tree rings as they grow. In contrast, the direct path coefficient w1 was, in general, significantly positive (w1 = 0.33), ranging from −0.006 (PER) to 0.82 (CCB) across sites (Figure 4a). This suggests that larger trees produce denser wood as trees become larger. No correlation was found between r1 and w1 (Figure S14C), indicating that long-term ontogenetic changes in TRW and WD, caused by tree size in diameter, were uncoupled along the environmental gradient.

The direct effect of TRW and WD on ABP_P was also significant (r2 and w2: r^2 cond. = 0.99, p-value < 0.001). The direct path coefficients r2 and w2 contributed, in general, positively to ABP_P (r2 = 0.69 and w2 = 0.09, Figure 4). However, w2 presented low variance in the standardised estimates across sites (Figure 4b), ranging from 0.07 (CVCE, p-value < 0.001) to 0.12 (LGT, p-value < 0.001). The standardised estimates across sites for r2 were approximately five times greater than w2, ranging from 0.56 (FNJ) to 0.85 (JU) across sites (Figure 4b). This result suggests that annual variation in TRW plays a variable but stronger role on ABP_P than annual variation in WD across sites. There was no significant correlation between r2 and w2 (Figure S14D), suggesting no coupling between interannual changes in TRW and WD along the environmental gradient.

The indirect effects of tree size on ABP_P, via TRW (r1 × r2) and WD (w1 × w2), reflected the direction of their respective direct effects (Figure 4c). The indirect effect of w1 × w2 was consistently positive, reflecting the combination of the positive influence from the long-term (w1) and short-term effects (w2). This effect was slightly stronger in humid sites, particularly in the Atlantic Forest (e.g. CCB, JU). In contrast, r1 × r2 was predominantly negative, driven by the combination of the negative long-term effect (r1) and the strong positive short-term effect (r2). Because r2 is substantially stronger than w2, the magnitude of r1 × r2 generally exceeded that of w1 × w2. This negative indirect effect was most pronounced in dry forests and transition zones (e.g. PER, BAH, CVCE) and parts of the Atlantic Forest (CCB, VRP), while it was close to zero in wetter Amazonian sites (e.g. FNJ, CNS). These patterns suggest that ontogenetic effects on ABP_P are primarily mediated by long-term changes in WD in wetter sites, whereas in drier regions, the annual effects on ABP_P are strongly driven by short-term changes in TRW. The same pattern of direct and indirect effect was observed considering ABP (Figures S12 and S13, Table S5).

The direct effect b1 was consistently negative across all sites (Figure 4d), with standardised estimates ranging from −0.53 (CCB) to −0.84 (ALT). This result indicates that larger trees contributed proportionally less to ABP_P over their lifespan. However, when considering absolute biomass production (ABP), b1 was consistently positive (Figures S12 and S13, Table S5), reflecting that, despite lower relative growth rates, larger trees accumulate greater total biomass over time.

13652745, 0, Downloaded from https://besjournals.onlinelibrary.wiley.com/doi/10.1111/1365-2745.70147 by Cochrane Peru, Wiley Online Library on [01/09/2025]. See the Terms and Conditions (https://onlinelibrary.wiley.com/terms-and-conditions) on Wiley Online Library for rules of use; OA articles are governed by the applicable Creative Commons License

BRITISH ECOLOGICAL SOCIETY Journal of Ecology

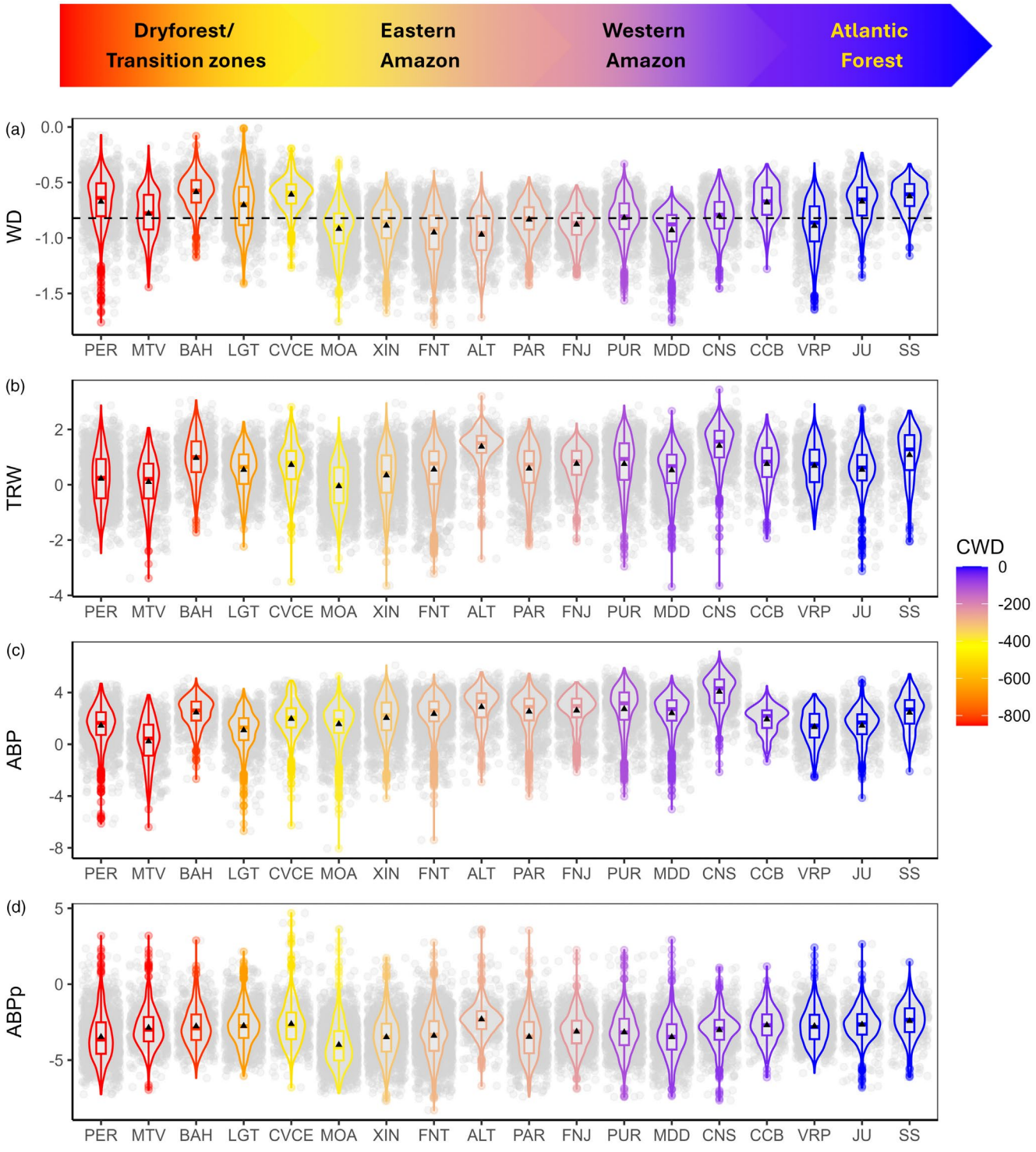

FIGURE 3 (a) tree-ring wood density in g/cm^3 (WD), converted to basic wood density by multiplying by 0.838 (Vieilledent et al., 2018); (b) tree-ring width in mm (TRW); (c) absolute annual biomass productivity in kg (ABP), calculated from Chave et al.'s (2014) pantropical equation across sites; and (d) annual relative biomass productivity (ABP_p). All variables were natural-log transformed. Sites are arranged from left to right by decreasing climatic water deficit (CWD from −800 to 0 mm, representing water stress, where more negative values indicate greater soil water deficit and higher stress for plants). CWD values close to zero represent the wettest forests. The black shape indicates the mean value. The dashed line represents the natural logarithm of 0.44 g/cm^3, indicating the mean wood density (g/cm^3) of *Cedrela fissilis* and *Cedrela odorata* in South America, obtained from a global wood density database (Zanne et al., 2009) and measured as oven-dry mass per fresh volume.

13652745, 0, Downloaded from https://besjournals.onlinelibrary.wiley.com/doi/10.1111/1365-2745.70147 by Cochrane Peru, Wiley Online Library on [01/09/2025]. See the Terms and Conditions (https://onlinelibrary.wiley.com/terms-and-conditions) on Wiley Online Library for rules of use; OA articles are governed by the applicable Creative Commons License

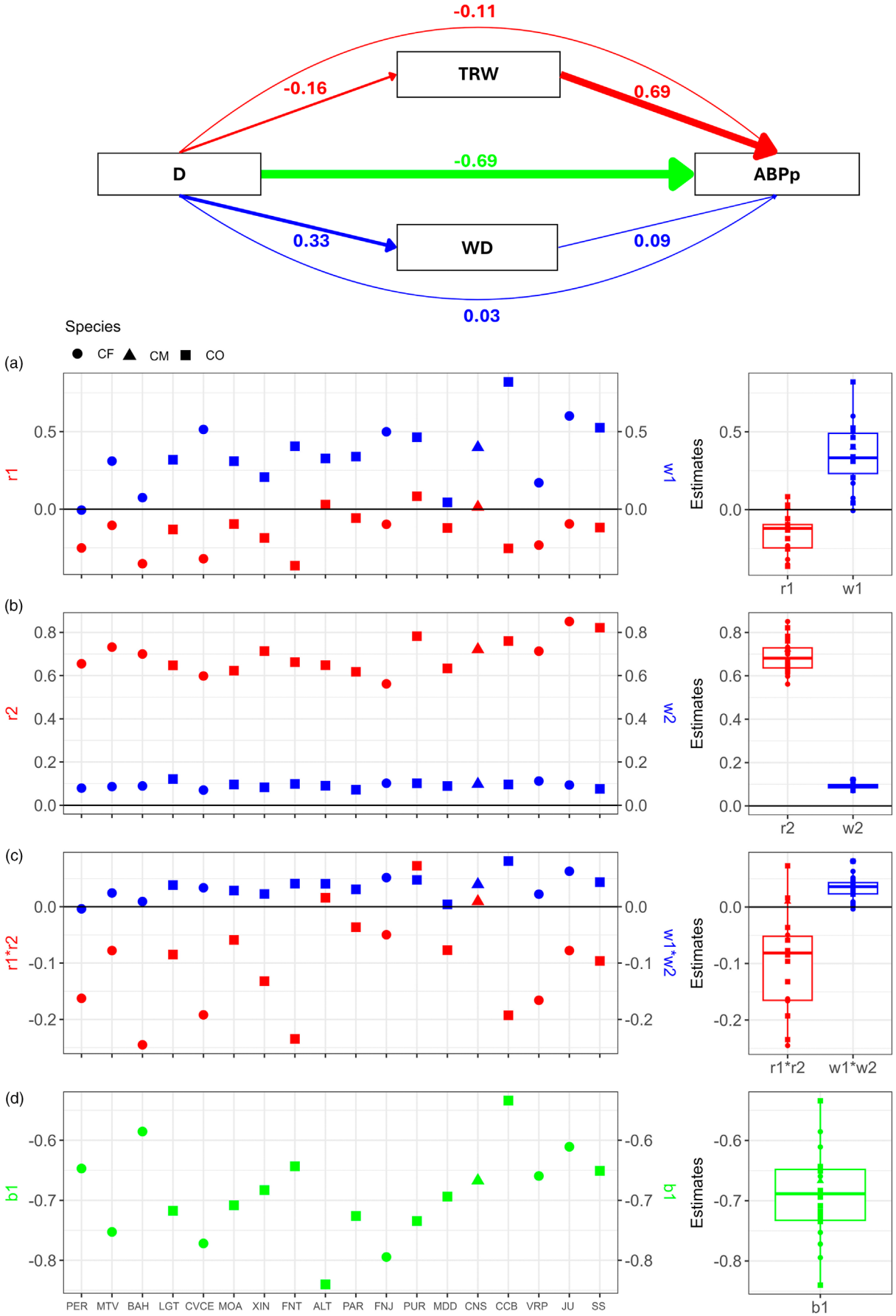

13652745, 0, Downloaded from https://besjournals.onlinelibrary.wiley.com/doi/10.1111/1365-2745.70147 by Cochrane Peru, Wiley Online Library on [01/09/2025]. See the Terms and Conditions (https://onlinelibrary.wiley.com/terms-and-conditions) on Wiley Online Library for rules of use; OA articles are governed by the applicable Creative Commons License

FIGURE 4 Structural diagram of the path analysis model showing general relationships between tree size (*D*), tree-ring width (TRW), wood density (WD) and relative biomass production (ABP_P). Arrows indicate standardised path coefficients extracted from the generalised linear mixed models (Equation 3), indicating the strength (slope) of the direct and indirect relationships. Direct effects represent the immediate influence of one variable on another (r1, r2, w1, w2, b1). Direct effect: (a) Standardised estimates of the path coefficients of r1 and w1 across study sites. (b) Standardised estimates of the path coefficients of r2 and w2 across study sites. (d) Standardised estimates of the path coefficients of b1 across study sites. Indirect effect: (c) Standardised estimates of the path coefficients of r1 × r2 and w1 × w2 for each site. Each left-side panel presents the standardised estimated path coefficients, illustrating the strength and significance of the relationship in each site (scatterplot), ordered according to the decreasing climatic water deficit (CWD from −800 to 0 mm, representing water stress, where more negative values indicate greater soil water deficit and higher stress for plants). Each right-side panel presents the standardised estimates in boxplots to represent the main direction of the effect (positive or negative). Species: *Cedrela fissilis* (CF), *Cedrela odorata* (CO) and *Cedrela montana* (CM).

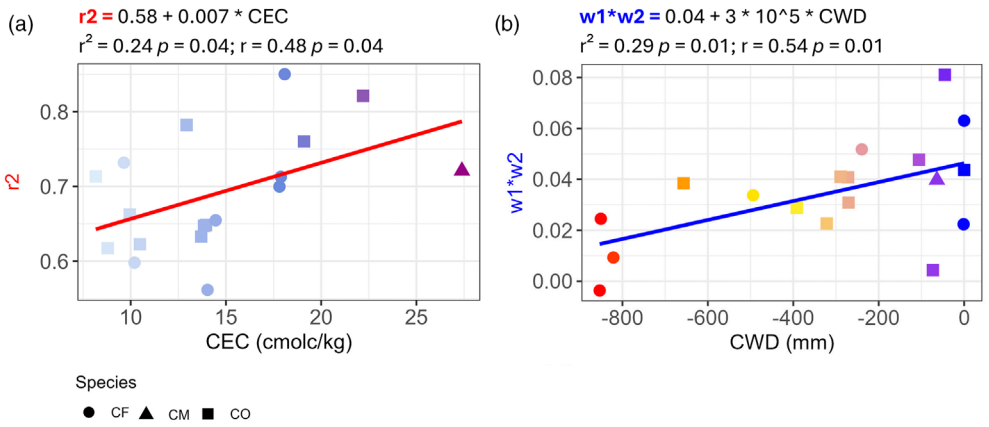

FIGURE 5 Linear relationship between cation exchange capacity (CEC) and climatic water deficit (CWD) with the strength of the standardised path coefficients of each site extracted from the generalised linear mixed models. The path coefficients showed a significant linear relationship between (a) the direct effect of tree-ring width on relative biomass production (r2) and CEC and (b) the tree size indirect effect via wood density on relative biomass production (w1 × w2) and CWD. The red and blue lines represent a significant linear regression ($p < 0.05$). Species: *Cedrela fissilis* (CF, circles), *Cedrela odorata* (CO, squares) and *Cedrela montana* (CM, triangles). Species colour represents the CWD and CEC gradient.

3.3 | Relationship of biomass production with climatic and soil characteristics

The direct effect w1 and indirect effect w1 × w2 presented a positive linear association with CWD (Figure 5, Figures S16 and S20). This indicates that in more humid environments (sites with lower CWD and VPD), the ontogenetic effect on WD has a positive contribution to ABP_P via WD. The direct effect r2 presented a positive linear association with CEC (Figures 5 and Figure S17) and a quadratic association with CWD (Figure S16). This suggests that the contribution of TRW to ABP_P is higher in more fertile soils and varies non-linearly along the CWD gradient. Specifically, the effect of TRW on ABP_P was higher in sites with either very low or very high CWD. A similar pattern was observed for ABP in relation to CWD (Figure S18), indicating that wetter sites not only support relative but also absolute biomass production. However, no significant relationship was found considering CEC (Figure S19).

4 | DISCUSSION

Here we evaluated how spatio-temporal variation in tree-ring width (TRW) and wood density (WD), driven by both ontogenetic (long-term) and interannual (short-term) factors, shape tree biomass production across a large environmental gradient. As expected, temporal variation in TRW and WD independently plays a significant role in biomass production, but their relative contributions differ depending on the timescale. TRW emerged as the dominant driver of short-term variation in biomass production, with WD playing a smaller role. Over the long term, ontogenetic changes in WD became the primary driver of biomass production, particularly in humid sites. Contrary to our expectation, only the ontogenetic effect via WD on biomass production was positively associated with water availability, indicating that long-term adjustments in WD play a crucial role in sustaining biomass production in wetter environments (Figure 6). These results highlight the importance of integrating both short-term variation in TRW and WD, as well as the critical role of long-term changes in WD, particularly in humid sites, to accurately capture biomass production dynamics across space and time.

4.1 | Interannual changes in tree biomass production

Short-term variation in TRW and WD positively contributed to annual biomass production. However, the direct effect of TRW on

13652745, 0, Downloaded from https://besjournals.onlinelibrary.wiley.com/doi/10.1111/1365-2745.70147 by Cochrane Peru, Wiley Online Library on [01/09/2025]. See the Terms and Conditions (https://onlinelibrary.wiley.com/terms-and-conditions) on Wiley Online Library for rules of use; OA articles are governed by the applicable Creative Commons License

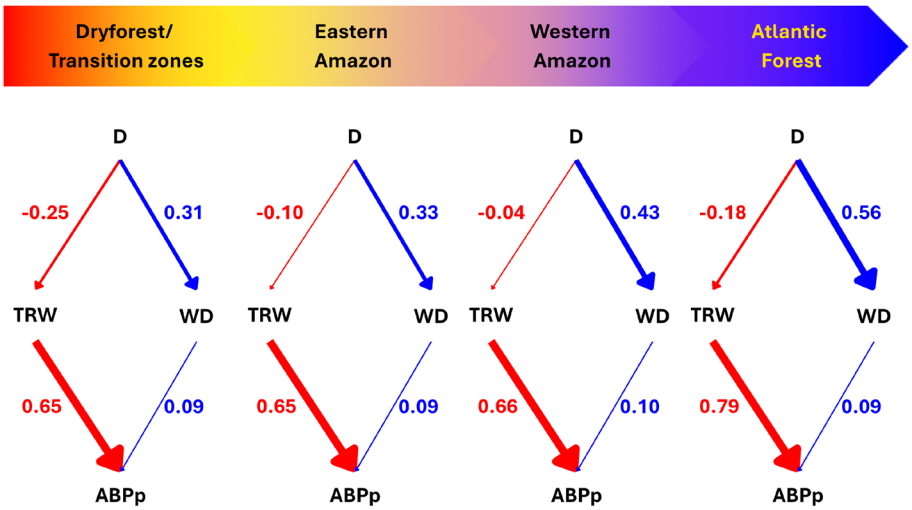

FIGURE 6 Structural diagram of the path analysis model showing general relationships between tree size (*D*), tree-ring width (TRW), wood density (WD) and relative biomass production (ABP_p) in the dry forest/transition zones ($n=5$ sites), the Eastern and Western Amazon Rainforest ($n=5$ and 4 sites, respectively) and the Atlantic Forest ($n=4$ sites). Arrows indicate mean standardised path coefficients extracted from the generalised linear mixed models (Equation 3), indicating the strength (slope) of the direct and indirect relationships. Values are the medians of the standardised path coefficients of each site extracted from the generalised linear mixed models. The size of the arrows represents the magnitude of the effect via WD (blue colour) and TRW (red colour). Grey arrows represent paths that are significant in some of the populations. The colour gradient red-yellow-blue represents the Climatic Water Deficit gradient from the driest to the wettest place (CWD near 0).

biomass production was, on average, five times stronger than that of WD, highlighting that diameter growth is the primary mechanism regulating year-to-year fluctuations in biomass production. This pattern is consistent with the large interannual variation in TRW observed in our data (up to 1000-fold within sites), contrasting with the substantially lower variability in WD (<6-fold changes within sites). Our findings are not surprising given that interannual variation in TRW of tropical tree species has often been reported to be high and strongly regulated by annual climatic fluctuation (Brienen et al., 2016; Schweingruber, 1989; Zuidema et al., 2022). In contrast, WD is commonly characterised by more pronounced low-frequency variation (Björklund et al., 2013; Schweingruber, 1989), potentially driven by genetic factors (e.g. Hylen, 1999; Louzada & Fonseca, 2002).

Although the contribution of WD to interannual biomass production was smaller, it was remarkably consistent across sites (Figures 4b and 6). These finds indicate that even subtle interannual fluctuations in WD can meaningfully affect biomass production and need attention. This is particularly relevant given that recent studies have shown that drought can induce shifts in annual WD in tropical trees (Ortega Rodriguez, Sánchez-Salguero, Hevia, Granato-Souza, Assis-Pereira, et al., 2023; Ortega Rodriguez, Sánchez-Salguero, Hevia, Granato-Souza, Cintra, et al., 2023), and much of our current knowledge about WD interannual variation comes from temperate species (Correa-Díaz et al., 2020; Olivar et al., 2015; Pompa-García et al., 2024). Together, these findings reinforce that WD variation, although limited, remains an important contributor to shaping biomass production.

4.2 | Ontogenetic changes in tree biomass production

Long-term ontogenetic changes in WD play an important positive role in shaping biomass production, particularly in humid sites, such as the Amazon rainforest and Atlantic Forest (Figures 4a and 6). This underscores the importance of structural adjustments in tissue density to maintain growth under favourable water conditions. The pattern likely reflects the greater mechanical, hydraulic and defensive demands (Philipson et al., 2014; Wright et al., 2010) along with increased respiratory and maintenance costs (Anten & Schieving, 2010), associated with the larger sizes attained by trees in humid forests compared to those in dry regions (Murphy & Lugo, 1986). For example, in dry environments, the limitation of tree height in *C. odorata* and *C. salvadorensis* is linked to smaller basal vessel sizes, which reduce embolism risk as an adaptive response to water stress (Chambers-Ostler et al., 2022).

In contrast, the ontogenetic effect via TRW was more evident in dry forest (Figures 4a and 6), where diameter growth declined with tree size. This pattern is likely attributable to the prolonged and severe drought conditions experienced by trees, leading to the rapid depletion of shallow water reserves and the reallocation of resources towards sustaining growth (Borchert, 1999). The rapid water storage traits, such as bark and wood structures, can be of great importance to ensure the functioning of many physiological processes, mainly for acquisitive species (Fagundes et al., 2022). During these processes, trees in dry forests may have low long-term variation in wood density to resist embolisms and maintain low vulnerability to drought across the tree's life (Janssen et al., 2020).

13652745, 0, Downloaded from https://besjournals.onlinelibrary.wiley.com/doi/10.1111/1365-2745.70147 by Cochrane Peru, Wiley Online Library on [01/09/2025]. See the Terms and Conditions (https://onlinelibrary.wiley.com/terms-and-conditions) on Wiley Online Library for rules of use; OA articles are governed by the applicable Creative Commons License

Surprisingly, we did not observe a consistent relationship between ontogenetic effect via TRW and WD, commonly reported for fast growth strategies (Chave et al., 2009; Hietz et al., 2013; Nock et al., 2009), as a strategic investment in enhanced structural strength at lower construction costs (Larjavaara & Muller-Landau, 2010). This suggests that the growth–density trade-off may be limited to specific life stages, environments or species.

These findings have direct implications for biomass estimation, particularly in humid forests. Relying on a single value (~0.43 g/cm^3) from a global wood density database for *C. fissilis* and *C. odorata* (Zanne et al., 2009) introduces systematic errors exceeding 20% between dry and humid sites (calculations shown in Supporting Information III). This leads to biomass overestimation for individuals in humid forests (especially between 10 and 20 cm in diameter in the Amazon forest) and an underestimation in dry forests throughout their adult stage. Incorporating ontogenetic WD variation into biomass models could significantly enhance their accuracy, mainly in humid sites.

However, while these ontogenetic effects are evident in fast-growing species like *Cedrela*, further research is needed to determine whether similar patterns occur in conservative species with slower growth rates and higher baseline WD, where wood density varies minimally with tree size (Bastin et al., 2015; González-Melo, 2021; Osazuwa-Peters et al., 2014).

4.3 | Environmental control of short and long-term biomass production

Water availability plays a central role in modulating long-term biomass production through its influence on wood density. This finding indicates that, although higher WD in dry forests provides mechanical and hydraulic resistance to drought, the investment in denser tissues becomes even more relevant in humid forests, where larger tree sizes demand greater structural support throughout ontogeny. This result offers a mechanistic explanation for macroecological patterns frequently reported in the tropics, where spatial variation in WD is strongly related to climate (Yang et al., 2024). Our findings suggest that the well-established relationship between water availability and biomass production (Becknell et al., 2012; Poorter et al., 2017; Souza et al., 2019) is, at least in part, mediated by ontogenetic adjustments in wood density in fast-growing species.

In contrast, water availability showed no significant effect when modulating long-term biomass production through its influence on diameter growth. This suggests that radial growth trajectories are less constrained by long-term climatic water balance but rather by annual climatic fluctuations (Brienen et al., 2016; Zuidema et al., 2022). However, we found that the direct effect of diameter growth on biomass production increased significantly with greater soil nutrient availability (high CEC). This indicates that, more than annual climate fluctuation, the soil fertility condition contributes more strongly to relative biomass production, likely reflecting the increased capacity for carbon allocation to stem growth when nutrient limitations are reduced (Van Der Sande et al., 2018).

Altogether, these findings show that environmental drivers distinctly influence the mechanisms behind biomass production. Water availability primarily shapes the long-term contribution of wood density, especially through ontogenetic changes, whereas soil fertility amplifies the direct contribution of radial growth to annual biomass accumulation. This dual environmental control reinforces the importance of integrating both climate and soil gradients when modelling biomass dynamics and carbon stocks in tropical forests.

5 | CONCLUSIONS

Our findings show that both wood density and diameter growth positively influence short-term variance in biomass output, but the effect of diameter is more pronounced and varied than that of wood density. Over time, we demonstrate that ontogenetic modifications in wood density, especially in humid environments, are more important than diameter expansion. Our results demonstrate the importance of considering both diameter growth and wood density when evaluating biomass and carbon storage across environmental gradients. Moreover, tropical trees face increasing impacts from climate change, including how long they can live and how they can grow in volume and wood density. Given the key role of wood density in driving tree biomass production, we suggest more studies quantify the amount of radial variation and wood density. Further, we recommend that biomass models and allometric equations be adapted to incorporate not only single-species estimates of wood density but also variation in radial wood density and climate to improve their accuracy.

AUTHOR CONTRIBUTIONS

Bruna Hornink, Pieter A. Zuidema, Peter van der Sleen, Peter Groenendijk and Amy E. Zanne conceived the study's conceptualisation. Bruna Hornink, Pieter A. Zuidema and Peter van der Sleen conducted the formal analysis. Bruna Hornink and Peter Groenendijk conducted the data curation. Bruna Hornink, Gabriel Assis-Pereira, Leif Armando Portal-Cahuana, Daigard Ricardo Ortega Rodriguez, Claudia Fontana, Claudio Sergio Lisi, Itallo Romany Nunes Menezes, Edilson Jimmy Requena-Rojas, Ana Carolina Maioli Campos Barbosa, Daniela Granato-Souza, Lucas Guimarães Pereira, Alejandro Venegas-Gonzalez, Fidel A. Roig, Mario Tomazello-Filho and Nelson Jaén-Barrios conducted the methodology. Peter Groenendijk and Mario Tomazello-Filho contributed with resources. Bruna Hornink wrote the original draft. All authors contributed critically to the drafts and gave final approval for publication.

AFFILIATIONS

[1]Department of Plant Biology, Institute of Biology, University of Campinas–UNICAMP, Campinas, São Paulo, Brazil; [2]Escola Superior de Agricultura Luiz de Queiroz, Department of Forest Resource, Universidade de São Paulo, Piracicaba, São Paulo, Brazil; [3]Forest Ecology and Forest Management Group, Wageningen University, Wageningen, The Netherlands; [4]Cary Institute of Ecosystem Studies, Millbrook, New York, USA; [5]Research and Development Department, Monte Verde Carbon, Itajubá, Minas

13652745, 0, Downloaded from https://besjournals.onlinelibrary.wiley.com/doi/10.1111/1365-2745.70147 by Cochrane Peru, Wiley Online Library on [01/09/2025]. See the Terms and Conditions (https://onlinelibrary.wiley.com/terms-and-conditions) on Wiley Online Library for rules of use; OA articles are governed by the applicable Creative Commons License

Gerais, Brazil; [6]Departamento Técnico-Científico, Instituto de Pesquisas Ambientais (IPA) do Estado de São Paulo, Assis, São Paulo, Brazil; [7]Instituto de Pesquisa em Florestas e Ecossistemas Tropicais (INIFET), Escola Profissional de Engenharia Florestal, Universidade Nacional Toribio Rodríguez de Mendoza de Amazonas, Chachapoyas, Amazonas, Peru; [8]Laboratorio de Dendrocronología, Universidad Continental, Urbanización San Antonio, Huancayo, Junín, Peru; [9]Dirección de Servicios Estratégicos Agrarios, Instituto Nacional de Innovación Agraria (INIA), Huancayo, Peru; [10]Department of Forest Science, Federal University of Lavras, Lavras, Minas Gerais, Brazil; [11]Department of Natural Resources and Environmental Sciences, Alabama A&M University, Huntsville, Alabama, USA; [12]Laboratory of Plant Anatomy and Dendroecology, Department of Biology, Federal University of Sergipe, São Cristóvão, Sergipe, Brazil; [13]Instituto de Ciencias Agroalimentarias, Animales y Ambientales (ICA3)-Universidad de O'Higgins, Santiago, Chile; [14]Facultad de Ciencias Naturales Exactas y Tecnología, Departamento de Botánica, Universidad de Panamá, Ciudad de Panamá, Panama; [15]Instituto Argentino de Nivología, Glaciología y Ciencias Ambientales, IANIGLA, Consejo Nacional de Investigaciones Científicas y Técnicas–CONICET, Mendoza, Argentina and [16]Hémera Centro de Observación de La Tierra, Escuela de Ingeniería Forestal, Facultad de Ciencias, Universidad Mayor, Huechuraba, Santiago, Chile

ACKNOWLEDGEMENTS

We thank the Wood Anatomy and Tree-Ring Laboratory (LAIM) (FAPESP project: 2009/53951-7), Department of Forest Sciences, Luiz de Queiroz College of Agriculture (ESALQ) and the Forest Ecology and Forest Management Group (FEM), Centre for Ecosystem Studies, Wageningen University, for all the technical and statistical support. This research was financed by the Post-Graduate Programme of Plant Biology (UNICAMP, Brazil), CNPq (number process: 160852/2022-6) and CAPES/PRINT (number process: 88887.975357/2024-00) grants. We also acknowledge financial support by the São Paulo Research Foundation, FAPESP (grants # 2023/14668-5 and 2020/01378-0 to GA; 2019/22516-5 and 2023/09253-0 to NJB; 2017/50085-3, 2018/22914-8 and 2023/07753-6 to DROR; Young Investigator Grant # 2018/01847-0 to PG). ACB thanks CNPq (grant# PQ 313129/2022-3). LGP thanks FAPEMIG (grant # APQ-01544-22). CF thanks FAPESP/CNPq (grants # 2024/02051-6 and 2024/14406-3). EJRR thanks ITTO (Fellowship Award grant 046/12S). CSL and IRNM thank the Universal Project CNPq (grant #403596/2023-8). The authors are also thankful for the field, laboratory and logistical support by the logging company Agrocortex Madeiras do Acre and Cooperativa Mista da Floresta Nacional do Tapajós. The Article Processing Charge for the publication of this research was funded by the Coordenação de Aperfeiçoamento de Pessoal de Nível Superior - Brasil (CAPES) (ROR identifier: 00x0ma614).

CONFLICT OF INTEREST STATEMENT

Peter Zuidema is an Associate Editor of *Journal of Ecology* but took no part in the peer review and decision-making processes for this paper.

PEER REVIEW

The peer review history for this article is available at https://www.webofscience.com/api/gateway/wos/peer-review/10.1111/1365-2745.70147.

DATA AVAILABILITY STATEMENT

Data are deposited in the Dryad Digital Repository: https://doi.org/10.5061/dryad.1g1jwsv9b (Hornink et al., 2025).

STATEMENT ON INCLUSION

Our study brings together authors from Brazil, Peru, Chile, USA and The Netherlands, including scientists based in the country where the study was conducted. All authors were engaged early on with the research to ensure that the diverse sets of perspectives they represent were considered from the onset. Whenever relevant, literature published by scientists from the region was cited.

ORCID

Bruna Hornink https://orcid.org/0000-0002-8765-540X
Alejandro Venegas-Gonzalez https://orcid.org/0000-0003-4568-4533
Peter Groenendijk https://orcid.org/0000-0003-2752-6195

REFERENCES

Abatzoglou, J. T., Dobrowski, S. Z., Parks, S. A., & Hegewisch, K. C. (2018). TerraClimate, a high-resolution global dataset of monthly climate and climatic water balance from 1958–2015. *Scientific Data*, *5*, 170191. https://doi.org/10.1038/sdata.2017.191

Andreacci, F., Botosso, P. C., & Galvão, F. (2017). Fenologia Vegetativa e Crescimento de *Cedrela fissilis* na Floresta Atlântica, Paraná, Brasil. *Floresta e Ambiente*, *24*, e20150241. https://doi.org/10.1590/2179-8087.024115

Anten, N. P. R., & Schieving, F. (2010). The role of wood mass density and mechanical constraints in the economy of tree architecture. *The American Naturalist*, *175*, 250–260. https://doi.org/10.1086/649581

Babst, F., Alexander, M. R., Szejner, P., Bouriaud, O., Klesse, S., Roden, J., Ciais, P., Poulter, B., Frank, D., Moore, D. J. P., & Trouet, V. (2014). A tree-ring perspective on the terrestrial carbon cycle. *Oecologia*, *176*, 307–322. https://doi.org/10.1007/s00442-014-3031-6

Baker, J. C. A., Santos, G. M., Gloor, M., & Brienen, R. J. W. (2017). Does Cedrela always form annual rings? Testing ring periodicity across South America using radiocarbon dating. *Trees*, *31*, 1999–2009. https://doi.org/10.1007/s00468-017-1604-9

Baker, T. R., Phillips, O. L., Malhi, Y., Almeida, S., Arroyo, L., Di Fiore, A., Erwin, T., Killeen, T. J., Laurance, S. G., Laurance, W. F., Lewis, S. L., Lloyd, J., Monteagudo, A., Neill, D. A., Patiño, S., Pitman, N. C. A., M. Silva, J. N., & Vásquez Martínez, R. (2004). Variation in wood density determines spatial patterns in Amazonian forest biomass. *Global Change Biology*, *10*, 545–562. https://doi.org/10.1111/j.1365-2486.2004.00751.x

Banin, L., Lewis, S. L., Lopez-Gonzalez, G., Baker, T. R., Quesada, C. A., Chao, K., Burslem, D. F. R. P., Nilus, R., Abu Salim, K., Keeling, H. C., Tan, S., Davies, S. J., Monteagudo Mendoza, A., Vásquez, R., Lloyd, J., Neill, D. A., Pitman, N., & Phillips, O. L. (2014). Tropical forest wood production: A cross-continental comparison. *Journal of Ecology*, *102*, 1025–1037. https://doi.org/10.1111/1365-2745.12263

Bastin, J. F., Fayolle, A., Tarelkin, Y., Van Den Bulcke, J., De Haulleville, T., Mortier, F., Beeckman, H., Van Acker, J., Serckx, A., Bogaert, J., & De Cannière, C. (2015). Wood specific gravity variations and biomass of central African tree species: The simple choice of the outer wood. *PLoS One*, *10*, 1–16. https://doi.org/10.1371/journal.pone.0142146

Bates, D., Mächler, M., Bolker, B., & Walker, S. (2015). Fitting linear mixed-effects models using lme4. *Journal of Statistical Software*, *67*, 1–48. https://doi.org/10.18637/jss.v067.i01

13652745, 0, Downloaded from https://besjournals.onlinelibrary.wiley.com/doi/10.1111/1365-2745.70147 by Cochrane Peru, Wiley Online Library on [01/09/2025]. See the Terms and Conditions (https://onlinelibrary.wiley.com/terms-and-conditions) on Wiley Online Library for rules of use; OA articles are governed by the applicable Creative Commons License

Bauman, D., Fortunel, C., Delhaye, G., Malhi, Y., Cernusak, L. A., Bentley, L. P., Rifai, S. W., Aguirre-Gutiérrez, J., Menor, I. O., Phillips, O. L., McNellis, B. E., Bradford, M., Laurance, S. G. W., Hutchinson, M. F., Dempsey, R., Santos-Andrade, P. E., Ninantay-Rivera, H. R., Chambi Paucar, J. R., & McMahon, S. M. (2022). Tropical tree mortality has increased with rising atmospheric water stress. *Nature*, *608*, 528–533. https://doi.org/10.1038/s41586-022-04737-7

Becknell, J. M., Kissing Kucek, L., & Powers, J. S. (2012). Aboveground biomass in mature and secondary seasonally dry tropical forests: A literature review and global synthesis. *Forest Ecology and Management*, *276*, 88–95. https://doi.org/10.1016/j.foreco.2012.03.033

Björklund, J. A., Gunnarson, B. E., Krusic, P. J., Grudd, H., Josefsson, T., Östlund, L., & Linderholm, H. W. (2013). Advances towards improved low-frequency tree-ring reconstructions, using an updated *Pinus sylvestris* L. MXD network from the Scandinavian Mountains. *Theoretical and Applied Climatology*, *113*, 697–710. https://doi.org/10.1007/s00704-012-0787-7

Borchert, R. (1999). Climatic periodicity, phenology, and cambium activity in tropical dry forest trees. *IAWA Journal*, *20*, 239–247. https://doi.org/10.1163/22941932-90000687

Brady, N. C., & Weil, R. R. (2016). *The nature and properties of soils, fifteenth edition, global edition*. Pearson Global Edition.

Bräuning, A., Volland-Voigt, F., Burchardt, I., Ganzhi, O., Nauss, T., & Peters, T. (2009). Climatic control of radial growth of *Cedrela montana* in a humid mountain rainforest in southern Ecuador. *Erdkunde*, *63*, 337–345. https://doi.org/10.3112/erdkunde.2009.04.04

Brienen, R. J. W., Schöngart, J., & Zuidema, P. A. (2016). Tree rings in the tropics: Insights into the ecology and climate sensitivity of tropical trees 439–461. https://doi.org/10.1007/978-3-319-27422-5_20

Brienen, R. J. W., Zuidema, P. A., & Martínez-Ramos, M. (2010). Attaining the canopy in dry and moist tropical forests: Strong differences in tree growth trajectories reflect variation in growing conditions. *Oecologia*, *163*, 485–496. https://doi.org/10.1007/s00442-009-1540-5

Canty, A., & Ripley, B. (1999). boot: Bootstrap Functions (Originally by Angelo Canty for S). https://doi.org/10.32614/CRAN.package.boot

Chambers-Ostler, A., Gloor, E., Galbraith, D., Groenendijk, P., & Brienen, R. (2022). Vessel tapering is conserved along a precipitation gradient in tropical trees of the genus Cedrela. *Trees*, *37*, 269–284. https://doi.org/10.1007/s00468-022-02345-6

Chave, J., Condit, R., Lao, S., Caspersen, J. P., Foster, R. B., & Hubbell, S. P. (2003). Spatial and temporal variation of biomass in a tropical forest: Results from a large census plot in Panama. *Journal of Ecology*, *91*, 240–252. https://doi.org/10.1046/j.1365-2745.2003.00757.x

Chave, J., Coomes, D., Jansen, S., Lewis, S. L., Swenson, N. G., & Zanne, A. E. (2009). Towards a worldwide wood economics spectrum. *Ecology Letters*, *12*, 351–366. https://doi.org/10.1111/j.1461-0248.2009.01285.x

Chave, J., Réjou-Méchain, M., Búrquez, A., Chidumayo, E., Colgan, M. S., Delitti, W. B. C., Duque, A., Eid, T., Fearnside, P. M., Goodman, R. C., Henry, M., Martínez-Yrízar, A., Mugasha, W. A., Muller-Landau, H. C., Mencuccini, M., Nelson, B. W., Ngomanda, A., Nogueira, E. M., Ortiz-Malavassi, E., … Vieilledent, G. (2014). Improved allometric models to estimate the aboveground biomass of tropical trees. *Global Change Biology*, *20*, 3177–3190. https://doi.org/10.1111/gcb.12629

Cooper, M., Mendes, L. M. S., Silva, W. L. C., & Sparovek, G. (2005). A National Soil Profile Database for Brazil available to international scientists. *Soil Science Society of America Journal*, *69*, 649–652. https://doi.org/10.2136/sssaj2004.0140

Correa-Díaz, A., Gómez-Guerrero, A., Vargas-Hernández, J. J., Rozenberg, P., & Horwath, W. R. (2020). Long-term wood micro-density variation in Alpine forests at Central México and their spatial links with remotely sensed information. *Forests*, *11*, 452. https://doi.org/10.3390/f11040452

Fagundes, M. V., Souza, A. F., Oliveira, R. S., & Ganade, G. (2022). Functional traits above and below ground allow species with distinct ecological strategies to coexist in the largest seasonally dry tropical forest in the Americas. *Frontiers in Forests and Global Change*, *5*, 930099. https://doi.org/10.3389/ffgc.2022.930099

Flores, T. B. (2021). *Meliaceae in Flora do Brasil 2020*. Jardim Botânico do Rio de Janeiro. http://floradobrasil.jbrj.gov.br/reflora/floradobrasil/FB9992

Fontana, C., López, L., Santos, G. M., Villalba, R., Hornink, B., Assis-Pereira, G., Roig, F. A., & Tomazello-Filho, M. (2024). A new chronology of *Cedrela fissilis* (Meliaceae) for southern Brazil: Combining classical dendrochronology and radiocarbon dating. *Dendrochronologia*, *85*, 126214. https://doi.org/10.1016/j.dendro.2024.126214

Fritts, H. C. (1976). Dendrochronology and dendroclimatology. In H. C. Fritts (Ed.), *Tree rings and climate* (pp. 1–54). Academic Press. https://doi.org/10.1016/b978-0-12-268450-0.50006-9

Gonçalves, J. Q., Durgante, F. M., Wittmann, F., Piedade, M. T. F., Ortega Rodriguez, D. R., Tomazello-Filho, M., Parolin, P., & Schöngart, J. (2021). Minimum temperature and evapotranspiration in Central Amazonian floodplains limit tree growth of Nectandra amazonum (Lauraceae). *Trees*, *35*, 1367–1384. https://doi.org/10.1007/s00468-021-02126-7

González-Melo, A. (2021). Radial variations in wood density, and their implications for above-ground biomass estimations, in a tropical high-andean forest. *Dendrobiology*, *86*, 19–29. https://doi.org/10.12657/denbio.086.003

Granato-Souza, D., Stahle, D. W., Barbosa, A. C., Feng, S., Torbenson, M. C. A., de Assis Pereira, G., Schöngart, J., Barbosa, J. P., & Griffin, D. (2019). Tree rings and rainfall in the equatorial Amazon. *Climate Dynamics*, *52*, 1857–1869. https://doi.org/10.1007/s00382-018-4227-y

Groenendijk, P., Babst, F., Trouet, V., Fan, Z.-X., Granato-Souza, D., Locosselli, G. M., Mokria, M., Panthi, S., Pumijumnong, N., Abiyu, A., Acuña-Soto, R., Adenesky-Filho, E., Alfaro-Sánchez, R., Anholetto Junior, C. R., Aragão, J. R. V., Assis-Pereira, G., Astudillo-Sánchez, C. C., Carolina Barbosa, A., Barreto, N. D. O., … Zuidema, P. A. (2025). The importance of tropical tree-ring chronologies for global change research. *Quaternary Science Reviews*, *355*, 109233. https://doi.org/10.1016/j.quascirev.2025.109233

Groenendijk, P., Bongers, F., & Zuidema, P. A. (2017). Using tree-ring data to improve timber-yield projections for African wet tropical forest tree species. *Forest Ecology and Management*, *400*, 396–407. https://doi.org/10.1016/j.foreco.2017.05.054

Hérault, B., Bachelot, B., Poorter, L., Rossi, V., Bongers, F., Chave, J., Paine, C. E. T., Wagner, F., & Baraloto, C. (2011). Functional traits shape ontogenetic growth trajectories of rain forest tree species. *Journal of Ecology*, *99*, 1431–1440. https://doi.org/10.1111/j.1365-2745.2011.01883.x

Hietz, P., Valencia, R., & Joseph Wright, S. (2013). Strong radial variation in wood density follows a uniform pattern in two neotropical rain forests. *Functional Ecology*, *27*, 684–692. https://doi.org/10.1111/1365-2435.12085

Hornink, B., Zuidema, P. A., van der Sleen, P., Zanne, A. E., Assis-Pereira, G., Ortega Rodriguez, D. R., Fontana, C., Portal-Cahuana, L. A., Requena-Rojas, E. J., Barbosa, A. C. M. C., Granato-Souza, D., Pereira, L. G., Lisi, C. S., Menezes, I. R. N., Venegas-Gonzalez, A., Jaén-Barrios, N., Roig, F. A., Tomazello-Filho, M., & Groenendijk, P. (2025). Data from: Biomass production of tropical trees across space and time: The shifting roles of diameter growth and wood density [dataset]. *Dryad*. https://doi.org/10.5061/dryad.1g1jwsv9b

Hylen, G. (1999). Age trends in genetic parameters of wood density in young Norway spruce. *Canadian Journal of Forest Research*, *29*, 135–143. https://doi.org/10.1139/x98-170

Janssen, T. A. J., Hölttä, T., Fleischer, K., Naudts, K., & Dolman, H. (2020). Wood allocation trade-offs between fiber wall, fiber lumen, and axial parenchyma drive drought resistance in neotropical trees.

13652745, 0, Downloaded from https://besjournals.onlinelibrary.wiley.com/doi/10.1111/1365-2745.70147 by Cochrane Peru, Wiley Online Library on [01/09/2025]. See the Terms and Conditions (https://onlinelibrary.wiley.com/terms-and-conditions) on Wiley Online Library for rules of use; OA articles are governed by the applicable Creative Commons License

Plant, Cell & Environment, *43*, 965–980. https://doi.org/10.1111/pce.13687

King, D. A., Davies, S. J., Nur Supardi, M. N., & Tan, S. (2005). Tree growth is related to light interception and wood density in two mixed dipterocarp forests of Malaysia. *Functional Ecology*, *19*, 445–453. https://doi.org/10.1111/j.1365-2435.2005.00982.x

Köhl, M., Neupane, P. R., & Lotfiomran, N. (2017). The impact of tree age on biomass growth and carbon accumulation capacity: A retrospective analysis using tree ring data of three tropical tree species grown in natural forests of Suriname. *PLoS One*, *12*, 1–17. https://doi.org/10.1371/journal.pone.0181187

Lachenbruch, B., & McCulloh, K. A. (2014). Traits, properties, and performance: How woody plants combine hydraulic and mechanical functions in a cell, tissue, or whole plant. *The New Phytologist*, *204*, 747–764. https://doi.org/10.1111/nph.13035

Larjavaara, M., & Muller-Landau, H. C. (2010). Rethinking the value of high wood density. *Functional Ecology*, *24*, 701–705. https://doi.org/10.1111/j.1365-2435.2010.01698.x

Lefcheck, J. S. (2016). piecewiseSEM: Piecewise structural equation modelling in r for ecology, evolution, and systematics. *Methods in Ecology and Evolution*, *7*, 573–579. https://doi.org/10.1111/2041-210X.12512

Locosselli, G. M., Brienen, R. J. W., de Souza Leite, M., Gloor, M., Krottenthaler, S., de Oliveira, A. A., Barichivich, J., Anhuf, D., Ceccantini, G., Schöngart, J., & Buckeridge, M. (2020). Global tree-ring analysis reveals rapid decrease in tropical tree longevity with temperature. *Proceedings of the National Academy of Sciences of the United States of America*, *117*, 33358–33364. https://doi.org/10.1073/PNAS.2003873117

López, L., & Fontana, C. (2024). A cross-biome analysis of *Cedrela fissilis* Vell: Growth, age, and diameter class transitions. *Trees, Forests and People*, *18*, 100666. https://doi.org/10.1016/j.tfp.2024.100666

Louzada, J. L. P. C., & Fonseca, F. M. A. (2002). The heritability of wood density components in *Pinus pinaster* Ait. and the implications for tree breeding. *Annals of Forest Science*, *59*, 867–873. https://doi.org/10.1051/forest:2002085

Marcati, C. R., Angyalossy, V., & Evert, R. F. (2006). Seasonal variation in wood formation of *Cedrela fissilis* (Meliaceae). *IAWA Journal*, *27*, 199–211. https://doi.org/10.1163/22941932-90000149

Martin, A. R., & Thomas, S. C. (2011). A reassessment of carbon content in tropical trees. *PLoS One*, *6*, e23533. https://doi.org/10.1371/journal.pone.0023533

Mendivelso, H. A., Camarero, J. J., Gutiérrez, E., & Castaño-Naranjo, A. (2016). Climatic influences on leaf phenology, xylogenesis and radial stem changes at hourly to monthly scales in two tropical dry forests. *Agricultural and Forest Meteorology*, *216*, 20–36. https://doi.org/10.1016/j.agrformet.2015.09.014

Menezes, I. R. N., Aragão, J. R. V., Pagotto, M. A., & Lisi, C. S. (2022). Teleconnections and edaphoclimatic effects on tree growth of *Cedrela odorata* L. in a seasonally dry tropical forest in Brazil. *Dendrochronologia*, *72*, 125923. https://doi.org/10.1016/j.dendro.2022.125923

Mitchard, E. T. A. (2018). The tropical forest carbon cycle and climate change. *Nature*, *559*, 527–534. https://doi.org/10.1038/s41586-018-0300-2

Mo, L., Crowther, T. W., Maynard, D. S., Van Den Hoogen, J., Ma, H., Bialic-Murphy, L., Liang, J., de-Miguel, S., Nabuurs, G.-J., Reich, P. B., Phillips, O. L., Abegg, M., Adou Yao, Y. C., Alberti, G., Almeyda Zambrano, A. M., Alvarado, B. V., Alvarez-Dávila, E., Alvarez-Loayza, P., Alves, L. F., … Zohner, C. M. (2024). The global distribution and drivers of wood density and their impact on forest carbon stocks. *Nature Ecology & Evolution*, *8*, 2195–2212. https://doi.org/10.1038/s41559-024-02564-9

Muller-Landau, H. C. (2004). Interspecific and inter-site variation in wood specific gravity of tropical trees. *Biotropica*, *36*, 20–32. https://doi.org/10.1111/j.1744-7429.2004.tb00292.x

Muniz, M., Curi, N., Sparovek, G., Carvalho Filho, A. D., & Godinho Silv, S. H. (2011). Updated Brazilian's georeferenced soil database—An improvement for international scientific information exchanging. In B. E. Ozkaraova Gungor (Ed.), *Principles, Application and Assessment in Soil Science*. InTech. https://doi.org/10.5772/29627

Murphy, P. G., & Lugo, A. E. (1986). Ecology of tropical dry forest. *Annual Review of Ecology and Systematics*, *17*, 67–88. https://doi.org/10.1146/annurev.es.17.110186.000435

Nakagawa, S., & Schielzeth, H. (2013). A general and simple method for obtaining R^2 from generalized linear mixed-effects models. *Methods in Ecology and Evolution*, *4*, 133–142. https://doi.org/10.1111/j.2041-210x.2012.00261.x

Nock, C. A., Geihofer, D., Grabner, M., Baker, P. J., Bunyavejchewin, S., & Hietz, P. (2009). Wood density and its radial variation in six canopy tree species differing in shade-tolerance in western Thailand. *Annals of Botany*, *104*, 297–306. https://doi.org/10.1093/aob/mcp118

Olivar, J., Rathgeber, C., & Bravo, F. (2015). Climate change, tree-ring width and wood density of pines in Mediterranen environments. *IAWA*, *36*, 257–269. https://doi.org/10.1163/22941932-20150098

Ortega Rodriguez, D. R., Sánchez-Salguero, R., Hevia, A., Granato-Souza, D., Assis-Pereira, G., Roig, F. A., & Tomazello-Filho, M. (2023). Long- and short-term impacts of climate and dry-season on wood traits of *Cedrela fissilis* Vell. in southern Brazilian Amazon. *Agricultural and Forest Meteorology*, *333*, 109392. https://doi.org/10.1016/j.agrformet.2023.109392

Ortega Rodriguez, D. R., Sánchez-Salguero, R., Hevia, A., Granato-Souza, D., Cintra, B. B. L., Hornink, B., Andreu-Hayles, L., Assis-Pereira, G., Roig, F. A., & Tomazello-Filho, M. (2023). Climate variability of the southern Amazon inferred by a multi-proxy tree-ring approach using *Cedrela fissilis* Vell. *Science of the Total Environment*, *871*, 162064. https://doi.org/10.1016/j.scitotenv.2023.162064

Osazuwa-Peters, O. L., Wright, S. J., & Zanne, A. E. (2014). Radial variation in wood specific gravity of tropical tree species differing in growth-mortality strategies. *American Journal of Botany*, *101*, 803–811. https://doi.org/10.3732/ajb.1400040

Pagotto, M. A., Menezes, I. R. N., Costa, C. M., Lisi, C. S., & Bräuning, A. (2021). Oxygen isotopes in tree rings of *Cedrela odorata* L. as an indicator of hydroclimate variations in a seasonally dry tropical forest in northeastern Brazil. *Trees*, *35* 2., 1889–1903. https://doi.org/10.1007/s00468-021-02158-z

Pan, Y., Birdsey, R. A., Phillips, O. L., Houghton, R. A., Fang, J., Kauppi, P. E., Keith, H., Kurz, W. A., Ito, A., Lewis, S. L., Nabuurs, G.-J., Shvidenko, A., Hashimoto, S., Lerink, B., Schepaschenko, D., Castanho, A., & Murdiyarso, D. (2024). The enduring world forest carbon sink. *Nature*, *631*, 563–569. https://doi.org/10.1038/s41586-024-07602-x

Pan, Y., Birdsey, R. A., Phillips, O. L., & Jackson, R. B. (2013). The structure, distribution, and biomass of the world's forests. *Annual Review of Ecology, Evolution, and Systematics*, *44*, 593–622. https://doi.org/10.1146/annurev-ecolsys-110512-135914

Pennington, T. D., Muellner, A. N., & Wise, R. (2010). Cedrela. 1941.

Peters, R. L., Groenendijk, P., Vlam, M., & Zuidema, P. A. (2015). Detecting long-term growth trends using tree rings: A critical evaluation of methods. *Global Change Biology*, *21*, 2040–2054. https://doi.org/10.1111/gcb.12826

Philipson, C. D., Dent, D. H., O'Brien, M. J., Chamagne, J., Dzulkifli, D., Nilus, R., Philips, S., Reynolds, G., Saner, P., & Hector, A. (2014). A trait-based trade-off between growth and mortality: Evidence from 15 tropical tree species using size-specific relative growth rates. *Ecology and Evolution*, *4*, 3675–3688. https://doi.org/10.1002/ece3.1186

Phillips, O. L., Sullivan, M. J. P., Baker, T. R., Monteagudo, A., Percy, M., Vargas, N., & Vásquez, R. (2019). Species matter: Wood density influences tropical forest biomass at multiple scales. *Surveys in Geophysics*, *40*, 913–935. https://doi.org/10.1007/s10712-019-09540-0

13652745, 0, Downloaded from https://besjournals.onlinelibrary.wiley.com/doi/10.1111/1365-2745.70147 by Cochrane Peru, Wiley Online Library on [01/09/2025]. See the Terms and Conditions (https://onlinelibrary.wiley.com/terms-and-conditions) on Wiley Online Library for rules of use; OA articles are governed by the applicable Creative Commons License

Poggio, L., De Sousa, L. M., Batjes, N. H., Heuvelink, G. B. M., Kempen, B., Ribeiro, E., & Rossiter, D. (2021). SoilGrids 2.0: Producing soil information for the globe with quantified spatial uncertainty. *The Soil*, *7*, 217–240. https://doi.org/10.5194/soil-7-217-2021

Pompa-García, M., Vivar-Vivar, E. D., Hornink, B., Martínez-Rivas, J. A., Ortega-Rodriguez, D. R., & Mario, T.-F. (2024). Tree-ring wood density reveals differentiated hydroclimatic interactions in species along a bioclimatic gradient. *Dendrochronologia*, *85*, 126208. https://doi.org/10.1016/j.dendro.2024.126208

Poorter, L., van der Sande, M. T., Arets, E. J. M. M., Ascarrunz, N., Enquist, B., Finegan, B., Licona, J. C., Martínez-Ramos, M., Mazzei, L., Meave, J. A., Muñoz, R., Nytch, C. J., de Oliveira, A. A., Pérez-García, E. A., Prado-Junior, J., Rodríguez-Velázques, J., Ruschel, A. R., Salgado-Negret, B., Schiavini, I., … Peña-Claros, M. (2017). Biodiversity and climate determine the functioning of neotropical forests. *Global Ecology and Biogeography*, *26*, 1423–1434. https://doi.org/10.1111/geb.12668

Quesada, C. A., Phillips, O. L., Schwarz, M., Czimczik, C. I., Baker, T. R., Patiño, S., Fyllas, N. M., Hodnett, M. G., Herrera, R., Almeida, S., Alvarez Dávila, E., Arneth, A., Arroyo, L., Chao, K. J., Dezzeo, N., Erwin, T., Di Fiore, A., Higuchi, N., Honorio Coronado, E., … Lloyd, J. (2012). Basin-wide variations in Amazon forest structure and function are mediated by both soils and climate. *Biogeosciences*, *9*, 2203–2246. https://doi.org/10.5194/bg-9-2203-2012

Quintilhan, M. T., Santini, L., Ortega Rodriguez, D. R., Guillemot, J., Cesilio, G. H. M., Chambi-Legoas, R., Nouvellon, Y., & Tomazello-Filho, M. (2021). Growth-ring boundaries of tropical tree species: Aiding delimitation by long histological sections and wood density profiles. *Dendrochronologia*, *69*, 125878. https://doi.org/10.1016/j.dendro.2021.125878

R Core Team. (2022). *R: A language and environment for statistical computing*. R Foundation for Statistical Computing.

Reich, P. B. (2014). The world-wide 'fast-slow' plant economics spectrum: A traits manifesto. *Journal of Ecology*, *102*, 275–301. https://doi.org/10.1111/1365-2745.12211

Schweingruber, F. H. (1989). *Tree rings basics and applications of dendrochronology*. Paper Knowledge. Toward a Media History of Documents. https://doi.org/10.1007/978-94-009-1273-1

Shipley, B. (2016). *Cause and correlation in biology: A User's guide to path analysis, structural equations and causal inference with R* (2nd ed.). Cambridge University Press. https://doi.org/10.1017/CBO9781139979573

Souza, D. G., Sfair, J. C., De Paula, A. S., Barros, M. F., Rito, K. F., & Tabarelli, M. (2019). Multiple drivers of aboveground biomass in a human-modified landscape of the Caatinga dry forest. *Forest Ecology and Management*, *435*, 57–65. https://doi.org/10.1016/j.foreco.2018.12.042

Tomazello Filho, M., Botosso, P. C., Lisi, C. S., & Roig, F. A. (2000). Potencialidade da família Meliaceae para dendrocronologia em regiões tropicais e subtropicais. In *Dendrocronología en América Latina* (pp. 381–431). Editorial de la Universidad Nacional de Cuyo.

Tomazello, M., Brazolin, S., Chagas, M. P., Oliveira, J. T. S., Ballarin, A. W., & Benjamin, C. A. (2009). Application of X-ray in nondestructive evaluation of Eucalypt wood. *Maderas, Ciencia Y Tecnología*, *10*, 139–149. https://doi.org/10.4067/s0718-221x2008000200006

Van Der Sande, M. T., Arets, E. J. M. M., Peña-Claros, M., Hoosbeek, M. R., Cáceres-Siani, Y., Van Der Hout, P., & Poorter, L. (2018). Soil fertility and species traits, but not diversity, drive productivity and biomass stocks in a Guyanese tropical rainforest. *Functional Ecology*, *32*, 461–474. https://doi.org/10.1111/1365-2435.12968

Venegas-González, A., Roig, F. A., Lisi, C. S., Junior, A. A., Alvares, C. A., & Tomazello-Filho, M. (2018). Drought and climate change incidence on hospot Cedrela forests from the Mata Atlântica biome in southeastern Brazil. *Global Ecology and Conservation*, *15*, e00408. https://doi.org/10.1016/j.gecco.2018.e00408

Vieilledent, G., Fischer, F. J., Chave, J., Guibal, D., Langbour, P., & Gérard, J. (2018). New formula and conversion factor to compute basic wood density of tree species using a global wood technology database. *American Journal of Botany*, *105*, 1653–1661. https://doi.org/10.1002/ajb2.1175

Wickham, H. (2016). *ggplot2: Elegant graphics for data analysis, use R!* Springer International Publishing.

Williamson, G. B., & Wiemann, M. (2010). Measuring wood-specific gravity…correctly. *American Journal of Botany*, *97*, 519–524. https://doi.org/10.3732/ajb.0900243

Wright, S. J., Kitajima, K., Kraft, N. J. B., Reich, P. B., Wright, I. J., Bunker, D. E., Condit, R., Dalling, J. W., Davies, S. J., Díaz, S., Engelbrecht, B. M. J., Harms, K. E., Hubbell, S. P., Marks, C. O., Ruiz-Jaen, M. C., Salvador, C. M., & Zanne, A. E. (2010). Functional traits and the growth–mortality trade-off in tropical trees. *Ecology*, *91*, 3664–3674. https://doi.org/10.1890/09-2335.1

Yang, H., Wang, S., Son, R., Lee, H., Benson, V., Zhang, W., Zhang, Y., Zhang, Y., Kattge, J., Boenisch, G., Schepaschenko, D., Karaszewski, Z., Stereńczak, K., Moreno-Martínez, Á., Nabais, C., Birnbaum, P., Vieilledent, G., Weber, U., & Carvalhais, N. (2024). Global patterns of tree wood density. *Global Change Biology*, *30*, e17224. https://doi.org/10.1111/gcb.17224

Zanne, A. E., Lopez-Gonzalez, G., Coomes, D. A., Ilic, J., Jansen, S., Lewis, S. L., Miller, R. B., Swenson, N. G., Wiemann, M. C., & Chave, J. (2009). Data from: Towards a worldwide wood economics spectrum. https://doi.org/10.5061/DRYAD.234

Zuidema, P. A., Babst, F., Groenendijk, P., Trouet, V., Abiyu, A., Acuña-Soto, R., Adenesky-Filho, E., Alfaro-Sánchez, R., Aragão, J. R. V., Assis-Pereira, G., Bai, X., Barbosa, A. C., Battipaglia, G., Beeckman, H., Botosso, P. C., Bradley, T., Bräuning, A., Brienen, R., Buckley, B. M., … Zhou, Z. K. (2022). Tropical tree growth driven by dry-season climate variability. *Nature Geoscience*, *15*, 269–276. https://doi.org/10.1038/s41561-022-00911-8

Zuidema, P. A., Baker, P. J., Groenendijk, P., Schippers, P., van der Sleen, P., Vlam, M., & Sterck, F. (2013). Tropical forests and global change: Filling knowledge gaps. *Trends in Plant Science*, *18*, 413–419. https://doi.org/10.1016/j.tplants.2013.05.006

Zuur, A., Ieno, E., Walker, N., Saveliev, A., & Smith, G. (2009). Mixed effects models and extensions in ecology with R. https://doi.org/10.1007/978-0-387-87458-6

SUPPORTING INFORMATION

Additional supporting information can be found online in the Supporting Information section at the end of this article.

Supporting InformationI (SI-I):

Table S1. Characteristics of the *Cedrela* spp. populations and their local characteristics.

Table S2. Geographical, climatic, and soil data for each of the study sites.

Figure S1. (A) tree-ring wood density in g/cm^3 (WD), converted to basic wood density by multiplying by 0.838 (Vieilledent et al., 2018); (B) tree-ring width in mm (TRW); (C) absolute annual biomass productivity in kg (ABP), calculated from Chave et al.'s (2014) pantropical equation, across sites; and (D) annual relative biomass productivity (ABPP).

Figure S2. Relationship between tree cumulative diameter (cm) and tree-ring wood density (WD, g/cm^3) across the different sites.

Figure S3. Relationship between tree cambial age (years) and tree-ring wood density (WD, g/cm3) across the different sites.

Figure S4. Relationship between tree cumulative diameter (cm) and tree-ring width (TRW, mm) across the different sites.

13652745, 0, Downloaded from https://besjournals.onlinelibrary.wiley.com/doi/10.1111/1365-2745.70147 by Cochrane Peru, Wiley Online Library on [01/09/2025]. See the Terms and Conditions (https://onlinelibrary.wiley.com/terms-and-conditions) on Wiley Online Library for rules of use; OA articles are governed by the applicable Creative Commons License

Figure S5. Relationship between tree cambial age (years) and tree-ring width (TRW, mm) across the different sites.

Figure S6. Relationship between tree cumulative diameter (cm) and biomass production (ABP, kg) across the different sites.

Figure S7. Relationship between tree cambial age (years) and biomass production (ABP, kg) across different sites.

Figure S8. Relationship between tree cumulative diameter (cm) and proportional change in biomass (ABPp:ABP(*t*)/BP(*t*-1)) across the different sites.

Figure S9. Relationship between tree cambial age (years) and proportional change in biomass (ABPp: ABP(*t*)/BP(*t*-1)) across different sites.

Table S3. Summary of the linear mixed-effects model relating log-transformed tree age (from pith to bark) to log-transformed stem diameter.

Figure S10. Relationship between tree cambial age (years) and increment in diameter (cm) across the different sites.

Figure S11. Relationship between tree cambial age (years) and cumulative diameter (cm) across different sites.

Table S4. Model comparison to select generalised linear mixed models with different fixed and random effects structures.

Table S5. General path coefficients from the structural equation model (SEM) showing the direct and indirect effects of diameter (*D*) on tree-ring width (TRW), wood density (WD), and annual biomass production (ABP or ABPp).

Figure S12. Structural diagram of the path analysis model, showing hypothesised relationships between tree size (*D*), tree-ring width (TRW), wood density (WD), and absolute biomass production (ABP_P).

Figure S13. Structural diagram of the path analysis model showing general relationships between tree size (*D*), tree-ring width (TRW), wood density (WD), and absolute biomass production (ABP).

Figure S14. Linear relationships between standardised path coefficients in the structural equation model, considering relative annual biomass production (ABPp).

Figure S15. Linear relationships between standardised path coefficients in the structural equation model, considering absolute annual biomass production (ABP).

Figure S16. Relationship between path coefficients in the structural equation model with climatic water deficit (CWD). Direct effect: Tree size.

Figure S17. Relationship between path coefficients in the structural equation model with cation exchange capacity (CEC).

Figure S18. Relationship between path coefficients in the structural equation model with climatic water deficit (CWD).

Figure S19. Relationship between path coefficients in the structural equation model with cation exchange capacity (CEC).

Figure S20. Bootstrap correlations between path coefficients and environmental variables with confidence intervals.

Figure S21. Bootstrap correlations between path coefficients and environmental variables with confidence intervals.

Supporting Information II (SI-II):

Figure S1. Partitioning of variance for tree-ring width (TRW), wood density (WD), absolute aboveground biomass production (ABP), and relative aboveground biomass production (ABP_P) in log scale.

Figure S2. Estimated marginal means (with 95% confidence intervals) of tree-ring width (TRW), wood density (WD), aboveground biomass production (ABP), and relative aboveground biomass production (ABP_P) in log scale across sites.

Figure S3. Estimated marginal means (with 95% confidence intervals) of tree-ring width (TRW), wood density (WD), aboveground biomass production (ABP), and relative aboveground biomass production (ABPp: ABP(*t*)/BP(*t*-1)) in log scale across sites.

Supporting Information III (SI-III):

Figure S1. Relative error in cumulative biomass estimates when considering radial variation in wood density versus literature-based wood density across diameter classes.

Figure S2. Relative error in cumulative biomass estimates when considering radial variation in wood density versus literature-based wood density across diameter classes.

How to cite this article: Hornink, B., Zuidema, P. A., van der Sleen, P., Zanne, A. E., Assis-Pereira, G., Ortega Rodriguez, D. R., Fontana, C., Portal-Cahuana, L. A., Requena-Rojas, E. J., Barbosa, A. C. M. C., Granato-Souza, D., Guimarães Pereira, L., Lisi, C. S., Menezes, I. R. N., Venegas-Gonzalez, A., Jaén-Barrios, N., Roig, F. A., Tomazello-Filho, M., & Groenendijk, P. (2025). Biomass production of tropical trees across space and time: The shifting roles of diameter growth and wood density. *Journal of Ecology*, *00*, 1–18. https://doi.org/10.1111/1365-2745.70147

13652745, 0, Downloaded from https://besjournals.onlinelibrary.wiley.com/doi/10.1111/1365-2745.70147 by Cochrane Peru, Wiley Online Library on [01/09/2025]. See the Terms and Conditions (https://onlinelibrary.wiley.com/terms-and-conditions) on Wiley Online Library for rules of use; OA articles are governed by the applicable Creative Commons License